UNIVERSITÀ DEGLI STUDI DI MILANO
FACOLTÀ DI SCIENZE E TECNOLOGIE

Dipartimento di Fisica
Corso di Laurea Magistrale in Fisica

Approximation of the $p_\perp$ distribution of colorless objects from soft resummation

PACS: 11.55.Bq, 12.38.Bx

Relatore: Dott. Stefano Forte

Correlatore: Dott. Giancarlo Ferrera

Tesi di Laurea di:
Simone Rota
Matr. n. 939637

Anno Accademico 2019-2020

And as we danced among the ashes of our lives
we laughed it off
and then we burnt our tiny worlds
and found the ocean just beyond those paper walls.

Radical Face

Contents

Introduction

In this thesis work we consider the transverse momentum spectrum for the production of a massive colorless object in hadron collisions, focusing our attention on the physically more relevant case of Higgs boson production in proton-proton collision. In particular we exploit the known analytic structure of the fixed order cross section in Mellin space to derive an approximation for the fixed order $p_\perp$ distribution from the resummed cross section in the threshold limit.

We study the following scattering process:

$$h_1 + h_2 \longrightarrow H + X \tag{0.0.1}$$

where the collision of two hadrons h_1 and h_2 produces one Higgs boson H together with some extra radiation X.

This is arguably the most important process being studied at hadron colliders such as LHC. Indeed, the proton-proton collision is the first process in which a signal directly attributable to the production of Higgs bosons has been measured[2].

Higgs' discovery has been a fundamental step in the study of high energy particles and, in general, for physics as a whole, providing the last necessary building block for a consistent Standard Model (SM) of particle physics. Therefore the importance of pursuing a high precision test of the Standard Model's Higgs against collider's data cannot be overstated.

In order to accomplish such a task one needs both high precision experimental data and reliable theoretical predictions for the process at hand. We will be concerned with the latter.

The simplest measurable quantity in a given scattering process involving the production of a given particle is the inclusive cross section. This is the total probability of finding the particle of interest in the final state of the scattering given a fixed initial state. The inclusive cross section has the largest possible statistics in a given experimental setting since it includes every possible final state containing the particle to be studied. On the other hand, differential cross sections are less inclusive and therefore have less statistics but can contain more information than their inclusive counterpart.

We consider the transverse momentum spectrum, also called $p_\perp$ distribution or $p_\perp$ differential cross section which we denote as:

$$\frac{d\sigma}{dp_\perp^2} = \frac{1}{m^2}\frac{d\sigma}{d\xi}, \qquad \xi \equiv \frac{p_\perp^2}{m^2} \tag{0.0.2}$$

where m is the mass of the particle of interest, in our case the Higgs boson, and $p_\perp$ is its transverse momentum with respect to the axis of collision of the two hadrons.

Standard cross section computations rely on a perturbative expansion in the coupling constant: as long as the coupling constant is less than 1, higher orders in this expansion are numerically less and less important and truncating the series after the first few terms should give a good approximation for the full cross section. Such an approximation is called *fixed order cross section* and is the main procedure for producing quantitative predictions from a QFT in high energy particle physics.

Fixed order calculations lose their predictive power if the coupling constant is not small (e.g. in the low energy region of QCD) and when the convergence of the perturbative series is spoiled by the presence of large terms of kinematical origin. These usually appear when a cross section depends on multiple energy scales: the dependence on the different scales is in the form of logarithms of the ratio of two scales, and when these are different from each other (in some kinematical region) the logarithms become large.

The latter happens during the fixed order computation of the cross section we are interested in. In the threshold region, when the center-of-mass energy of the initial state is barely enough to produce one Higgs boson with a certain transverse momentum $p_\perp$ (and some radiation needed to recoil against it) the fixed order cross section contains terms like $\ln(1-x)$ where $x = Q^2/s$ is the ratio of the invariant mass of the final state and the initial state center-of-mass energy. These logarithms are due to gluon emission and become large when $Q^2 \simeq s$, i.e. in the threshold limit.

Those logarithms appear at all orders in the perturbative expansion of the cross section and spoil its convergence. As a result, in the threshold region standard perturbative approaches are not reliable and a procedure that consistently takes into account these logarithmic terms is needed.

A proper treatment of the logarithmic contributions is provided by resummation theory. This amounts to the classification of these terms in a hierarchy, followed by the summation of all the logarithms in a given hierarchy level. The result of this procedure is again a perturbative approximation of the cross section (albeit derived from a different power expansion) which does not contain any logarithmic term, and therefore properly regularizes the threshold logarithms.

The resummed cross section provides a reliable result in the kinematical region where the logarithmic terms that are resummed are actually big. In other kinematical regions the resummed cross section is not reliable and needs to be matched with the corresponding fixed order result to give an overall acceptable prediction.

The faulty behavior of the resummed cross section far away from the relevant kinematical limit is due to the fact that only the most divergent terms are considered in the resummation process, while all of the subleading contributions are disregarded. This blatantly manifests itself in the analytic structure of the cross section in Mellin space: the resummed cross section (when expanded at fixed order) presents cut singularities caused by $\ln(N)$ terms while the fixed order counterpart has pole singularities.

The objective of this thesis is to exploit the all-order information contained in the resummed cross section to provide an approximation for the fixed order $p_\perp$-spectrum. This is achieved by identifying the terms that generate the logarithms in the fixed order result: these reproduce the correct threshold behavior of the cross section while still manifesting the correct analytic structure. Once identified, their substitution in spite of the $\ln(N)$ in the resummed cross section provides the desired approximation.

This approximation is expected to reproduce the correct threshold behavior of the cross section at any fixed order while also being fairly reliable far from the threshold region. In particular, we expect it not to introduce any artificial divergences at low N.

Chapter 1

QCD and Resummation in a nutshell

This chapter is devoted to a quick overview over basic QCD concepts and resummation theory. It does not by any means try to encompass all of the knowledge that is present in the literature about these subjects, neither should it be viewed as a complete review of these theories. Nevertheless I will try to be as self-contained as possible, at least conceptualwise, and will aim at highlighting the main features that are necessary to ground the original work of this thesis.

1.1 QCD in the Standard Model

Quantum Chromo Dinamics (QCD for short) is the theory that describes the strong interaction in the context of the Standard Model of particle physics (SM). It is widely used in the study of particle collisions involving hadrons in the initial and/or final state, allowing the computation of quantum corrections for the related measurable quantities.

QCD is a $SU(3)$ gauge theory whose radiation modes (the gauge bosons) are called gluons; these live in the adjoint representation of $SU(3)$ and come in 8 possible color combinations. The matter fields that are subject to the strong interaction are the quarks, which live in the fundamental representation of $SU(3)$ and carry a $SU(3)$ charge called *color*. Up to now six *flavors* of quarks are known (together with the corresponding anti-quarks) which are classified in three families, each containing one quark of electrical charge $\frac{2}{3}$ and one of electrical charge $-\frac{1}{3}$[1].

[1] In this work the electrical charges are always written in units of the electron's charge e.

flavor	u “up”	d “down”	c “charme”	s “strange”	t “top”	b “bottom”
charge	2/3	-1/3	2/3	-1/3	2/3	-1/3
mass	∼2.5 MeV	∼5 MeV	1.3 GeV	0.1 GeV	4.2 GeV	173 GeV

Table 1.1: *The six known quarks with corresponding electric charges in units of* e *and masses in the* $\overline{MS}$ *scheme.*

The six known quarks, with corresponding electrical charge and mass, are listed in table 1.1.

1.1.1 Asymptotic freedom and confinement in QCD

The computation of transition amplitudes with QCD quantum corrections involves loop integrations that diverge. The UV divergences (i.e. the ones appearing when integrating over high energy momenta in a loop) can be regularized through the renormalization process. A side effect of renormalization, analogous to what happens in Quantum ElectroDinamics (QED), is the running of the strong coupling constant α_s described by the Callan-Symanzik equation (or RG equation):

$$\mu^2 \frac{d}{d\mu} \alpha_s(\mu^2) = \beta(\alpha_s(\mu^2)) \tag{1.1.1}$$

where β admits a perturbative expansion in the coupling constant[1]:

$$\beta = -\alpha_s^2(\beta_0 + \beta_1 \alpha_s + ...) \tag{1.1.2}$$

The leading coefficient is:

$$\beta_0 = \frac{11C_A - 2n_f}{12\pi} \tag{1.1.3}$$

which is positive for $n_f < 17$. This is actually the case since n_f is the number of (active) quark flavors and so far only six flavors are known to exist. Therefore the function β expanded to second order in (1.1.2) is negative and the perturbative Callan-Symanzik equation implies that α_s *decreases* as the energy scale *increases*.

There are two main consequences of the running of α_s, namely *confinement* and *asymptotic freedom*.

[1] While this is the most common expansion for the β-function we will be using different convention throughout this work in an attempt to adhere to the literature we refer to. Every time we introduce a new convention or present some result, we will make sure to explicit the convention we are using.

The property of asymptotic freedom states that, since the coupling constant becomes smaller and smaller as μ increases, then the intensity of the strong interaction dies off at high energies and in the high energy limit the colored particles are essentially free (non interacting). The only caveat to this thought process is the following: since the perturbative expansion of β is only valid when α_s is "small" the line of reasoning that leads to asymptotic freedom needs a "starting point" from which to take off. On the other hand, once a certain energy scale is found to exhibit a low intensity strong interaction, therefore rendering a perturbative approach viable, we are guaranteed that the coupling constant will decrease as we increase the energy. Moreover, the perturbative approach will continue to be valid at higher energies as α_s only gets smaller, enabling us to iterate the same reasoning over and over and leading us to asymptotic freedom.

The property of confinement states that, since the intensity of the strong interaction increases at low energies, the only propagating particles are white (with no color charge), i.e. the colored quarks and gluons are *confined* inside white bounded states. For the same perturbative nature that limited the discussion about asymptotic freedom, the treatment of confinement from an *a priori* prospective is not that simple either. Indeed, a full theoretical proof of QCD confinement is not available. The reason for this is that as the coupling constant gets larger with decreasing energies it eventually "exits the perturbative regime" and we are not able to make any claim about the behavior of the constant itself anymore. Nevertheless, we may make the statement that *the running of the QCD coupling constant, as computed via perturbative expansions, is compatible with the property of confinement.*

If we insist in computing the running coupling through the perturbative Callan-Symanzik equation, using for example as initial condition the measured value of α_s at the energy scale of the mass of the Z boson, we find that it diverges at some energy scale Λ. This scale is usually referred to as the Landau pole and denoted with Λ_{QCD} and it can be thought of as an indicative scale at which the strong interaction can no longer be treated perturbatively. The specific value of Λ_{QCD} varies with the perturbative order used throughout the computation and the renormalization scheme adopted, but is usually around a few hundreds MeV.

The property of confinement is phenomenologically observed, indeed it might be the most evident aspect of strong interaction: no colored particle nor long distance strong interaction is observed in nature. The colored matter and radiation particles only appear in nature as components of "larger", composite white particles: the hadrons. We will be focused on the proton since we are primarily interested in providing theoretical predictions for the LHC, which is a proton-proton collider; other hadrons include the neutron, the mesons (pions, kaons...) and heavy barions. The hadrons are bounded states kept together by strong interaction, although a theoretical-based description of the low energy dynamics that achieve this effect is not available.

1.1.2 The parton model

Even if a complete description of the structure of the hadrons is missing, one is interested in studying phenomena including them: for example an effective description of the behavior of protons undergoing collisions is desirable. This description is provided by the parton model, which models the hadrons as made up of its elementary constituents (partons), each carrying a fraction of the hadron's momentum z_i:

$$p_i = p_h z_i, \tag{1.1.4}$$

The partons' momenta are not fixed: rather we expect each parton to have a certain probability to be found with a fraction z_i of the hadron's momentum. This is modeled by a probability distribution $f_i(z_i)$, one for each parton type, called the *parton distribution functions* (PDFs). Then a cross section involving one hadron h in the initial state is assumed to be the incoherent sum of the hadron's partons' cross sections, also called partonic cross sections, weighted by the corresponding PDFs:

$$\sigma(p_h) = \sum_i \int_0^1 dz_i f_i(z_i) \hat{\sigma}_i(z_i p_h) \tag{1.1.5}$$

This is a naïve model as it does not take quantum corrections into account. In particular, QCD cross sections in the massless approximation (adopted in the context of the parton model) show infrared divergences which do not completely cancel between virtual and real emission diagrams. We won't go in more details regarding this issue, let us just mention that the collinear singularities emerging from QCD quantum corrections have to be regularized. This is achieved via the renormalization of the parton density functions, similar to the coupling constant renormalization necessary to regularize UV divergences. Indeed, the PDFs are not theoretically derived, as already discussed, and must be fitted to experimental data in order to make the parton model (1.1.5) useful. The newly defined PDFs acquire a scale dependence, as is usual with renormalization.

This *improved parton model* enables us to express the hadron's cross sections in terms of the partonic counterparts:

$$d\sigma_{h_1 h_2} = \sum_{a_1, a_2} \iint_0^1 dx_1 dx_2 f_{a_1/h_1}(x_1, \mu_F) f_{a_2/h_2}(x_2, \mu_F) d\hat{\sigma}_{a_1 a_2} \tag{1.1.6}$$

Equation (1.1.6) is usually called *QCD factorization theorem.* As already stated, the PDFs $f_{a_i/h_j}(z_i)$ describing the probability of finding a parton a_i in the hadron h_j with momentum fraction z_i are experimentally determined, while the partonic cross section $d\hat{\sigma}_{a_1 a_2}$ can be safely computed via perturbation theory, as will be described in the next section.

Finally, μ_F is the arbitrary energy scale introduced during the process of factorization, and is called *factorization scale.*

1.2 Fixed order computations in QFT

The main procedure to perform quantitative computations in an interacting Quantum Field Theory (QFT) is the fixed order expansion. This amounts to expanding the desired quantity to be computed (e.g. a cross section) as a power series in the coupling constant of the theory α, then retaining only the first few orders. If α is "small", namely substantially smaller than 1, then each term in the expansion becomes less and less important as the order grows and, at least from a naïve comparison of the various order, can be disregarded.

If all of these assumptions turn out to be true, then the result of this procedure is an approximation to the full quantity that one wishes to compute. Assuming that the perturbative expansion described above is well behaved, than the fixed order approximation gets closer and closer to the true value of the desired quantity the more terms one includes in the calculation.

Mathematically speaking this simply amounts to writing some quantity $R(\alpha)$ as:

$$R(\alpha) = \sum_{k=0}^{\infty} \alpha^k R_k \tag{1.2.1}$$

where R_k are some coefficient which does not depend on α. Then one can formally write:

$$R(\alpha) = \sum_{k=0}^{n} \alpha^k R_k + \mathcal{O}(\alpha^{m+1}) \tag{1.2.2}$$

and, assuming $\alpha < 1$, the $\mathcal{O}(\alpha^{m+1})$ may be discarded without spoiling the result too much. The result is called fixed order result, and throughout this thesis we will denote it with a fix subscript[1]:

$$R^{fix}(\alpha) \equiv \sum_{k=0}^{n} \alpha^k R_k \simeq R(\alpha) \tag{1.2.3}$$

This last step can obviously be justified only if one knows the values of the $\mathcal{O}(\alpha^{m+1})$ terms. This is usually not the case since one generally is only able to compute some of the terms in the expansion (1.2.1); the power series is then *assumed* to behave well under truncation at any arbitrary order.

This constitutes both the weakness and the main strength of fixed order calculations. On the one hand one is never able to compute the true value of the quantity he is interested in, and can only hope that his fixed order result will reproduce it well enough. On the other hand, the computation of some of the R_k coefficients will provide a concrete physical prediction for R, which may not be available otherwise. Practically speaking, any given quantity R is treated with a *presumption of convergence* and computed via a fixed order approximation, while alternative provisions are applied if it shows terms that spoil the convergence of its perturbative expansion.

1.2.1 Nomenclature

In this subsection we fix some notation used to refer to fixed order quantities. The first non-zero (and non-trivial) term in the perturbative expansion (1.2.1) is called *leading order* (LO), while the following terms are consequently denoted as *next-to-leading order*, *next-to-next-to-leading order* and so on.

Which term actually constitutes the *leading order* is sometimes not clear and should always be specified. For example, in the partonic cross section for Higgs production via gluon fusion the first non-zero term in the expansion is the one where two incoming gluons collide and (via a quark loop) produce one Higgs boson with no additional radiation. This term is proportional to α_s^4 and constitutes the *leading order* of the inclusive cross section:

$$\sigma_{gg\to H}(\alpha_s) = \sigma_{gg\to H}^{LO}\alpha_s^4 + \sigma_{gg\to H}^{NLO}\alpha_s^5 + \mathcal{O}(\alpha_s^6) \qquad (1.2.4)$$

On the other hand when considering the $p_\perp$ distribution for the same process this term is not generally considered since the kinematical constraints (namely the 4-momentum conservation) forces the transverse momentum of the Higgs boson to vanish. The $\mathcal{O}(\alpha_s^4)$ term in the $p_\perp$ spectrum is therefore proportional to $\delta(p_\perp)$ and has a trivial distribution.

For this reason the *leading order* of the $p_\perp$ distribution is generally considered to be the $\mathcal{O}(\alpha_s^6)$ term, and the perturbative expansion of the distri-

[1] We may occasionally drop the subscript when the context makes its use superfluous, and the fixed order nature of some quantity is obvious.

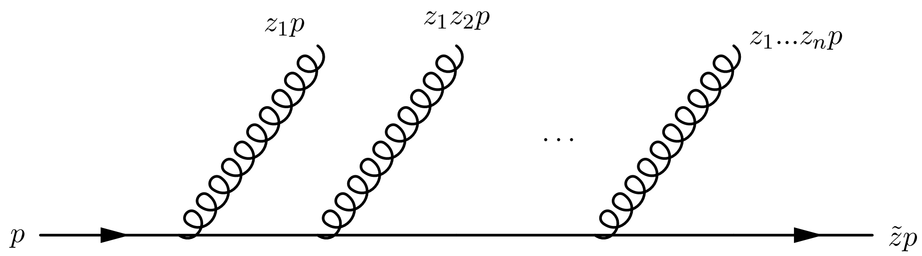

Figure 1.1: *Emission of multiple gluons from a single line. After N emissions the incoming particle is left with a fraction $\tilde{z} = z_1 z_2 ... z_n$ of its initial momentum*

bution is written as:

$$\frac{d\sigma_{gg\to H}(\alpha_s)}{dp_\perp^2} = \frac{d\sigma^{LO}_{gg\to H}}{dp_\perp^2}\alpha_s^6 + \frac{d\sigma^{NLO}_{gg\to H}}{dp_\perp^2}\alpha_s^7 + \mathcal{O}(\alpha_s^8) \tag{1.2.5}$$

1.3 Large logarithms - the Uprising

Let us now discuss a particular instance where, despite the coupling constant being small, the standard perturbative expansion is not well behaved and the fixed order result is unreliable in a specific kinematical region.

Consider the production of a system S with squared invariant mass M^2 within a gauge theory such as QED or QCD. The inclusive cross section $sigma(\alpha, z)$ will depend on the adimensional variable z defined as:

$$z = \frac{M^2}{s} \tag{1.3.1}$$

where s is the center-of-mass energy square of the incoming particles.

Suppose the cross section admits a power series expansion (for QCD scattering processes this will be true for the partonic cross section):

$$\sigma(\alpha, z) = \sum_{k=0}^{\infty} C_k(z)\alpha_s^k \tag{1.3.2}$$

The coefficients C_k will be kinematically enhanced when $z \to 1$ due to the emission of soft photons (or gluons). Indeed, the coefficients C_k with $k > 1$ will contain Feynman diagrams with multiple gauge boson emissions from the particles involved in the scattering process. Each emission carries an energy fraction $1 - z_i$ of the emitting particle; after n emissions the original particle's energy will be a fraction $\tilde{z} = z_1 z_2 ... z_n$ of its initial value.

Upon integration over the phase space of the emitted bosons these emissions will give rise in the coefficient C_k to terms proportional to:

$$\frac{\ln^m(1-z)}{1-z} \qquad\qquad 0 \leq m \leq 2k-1 \tag{1.3.3}$$

These terms are logarithmically enhanced in the threshold ($z \to 1$) region and are present at all orders in the perturbative expansion. In the case of a QCD partonic cross section the region $z \simeq 1$ is always encountered during the convolution of the cross section itself with the PDFs (1.1.6).

Therefore when z is such that:

$$\alpha_s \ln(1-z) \sim 1 \tag{1.3.4}$$

all the terms proportional to $(\alpha_s \ln(1-z))^k$ are roughly of the same magnitude and any fixed order truncation would not be justifiable.

Therefore the presence of these logarithmic contributions spoils the fixed order result in the threshold region and renders the fixed order cross section unreliable. This makes the need to find an alternative way of computing this cross section evident and is the primary motivation for the resummation procedure.

Resummation theory enables us to include the logarithmic contributions at all orders by providing an alternative perturbative expansion of the cross section that produces reliable results when truncated. This is accomplished by factorizing and then exponentiating the contributions from real soft emission[20]; the result is a perturbative expansion in α with $\alpha \ln(1-x)$ fixed (formally $\alpha \ln(1-x)$ is considered of order unity). Loosely speaking each “large” logarithm is paired with a “small” coupling constant and what is left is not affected by large kinematical terms anymore.

1.4 Large logarithms - the Factorization

The possibility of obtaining a finite, reliable result even when large logarithms appear is due to the fact that the perturbative series has to converge to the true cross section when all the perturbative terms are included. The large logarithms are just an artifact of the fixed order truncation and should sum to a physically acceptable result if we were able to take into account their contribution at all orders.

The first step in this direction is the factorization of the soft (and collinear) contributions to the cross section. In order to achieve this, one has to be able to factorize both the phase space and the matrix element of a given cross section.

While the phase space factorization depends on the particular process at hand, the matrix element always factorizes in the soft and/or collinear limit. In this section I give a brief overview over this universal factorization of QCD matrix elements in order to justify, at least conceptually, the resummation procedure and its reliability in the appropriate limit.

1.4.1 Weinberg soft photon theorem

Let us first consider the simpler example of QED soft emission. I will present a simple proof of soft matrix element factorization following a paper from Weinberg[17]. Although this does not include collinear emissions, which needs to be considered when computing a QCD cross section[1], it represents a fairly general statement about soft emission. Indeed, this same proof can be applied to gauge theories (both abelian and Yang-Mills), gravity and a variety of other theories[18].

Consider a tree level process with N external legs of momenta $p_i, i = 1, 2, ..., N$ and spin 0. Attaching a photon of momentum q to the $i-$th leg accounts to adding a vertex factor and a propagator of momentum $p + \eta q$ to the matrix element.

Overall this gives a factor:

$$\frac{e_i(2p_i^\mu + \eta_i q^\mu)}{(p_i + \eta_i q)^2 + m_i^2 - i\varepsilon} \tag{1.4.1}$$

where $\eta = \pm 1$ depending on whether the $i-$th particle is incoming or outgoing and m_i is the mass of said particle. In the limit $q \to 0$ this factor becomes

$$\frac{e_i \eta_i p_i^\mu}{p_i \cdot q - i\eta_i\varepsilon} \tag{1.4.2}$$

While Eq. (1.4.2) is only true for spin-0 hard particles, the soft version Eq. (1.4.3) holds for any spin[17].

Attaching the photon to an internal line will give contributions that are negligible in the soft limit, since they lack the $p \cdot q$ factor in the denominator. Therefore we only need to consider the diagrams where the photon is attached to an external line; adding all these together, we find that the

[1] More on this in the remarks at the end of this Section.

factor acquired when emitting a soft photon is:

$$\sum_{i=1}^{N} \frac{e_i \eta_i p_i^\mu}{p_i \cdot q - i\eta_i \varepsilon} \tag{1.4.3}$$

If the emission of multiple soft photons is considered, it turns out[17] that we simply get the product of several factors of the form (1.4.2), one for each emitted photons.

When computing an amplitude that contains soft photon emissions we can therefore approximate it by the tree level amplitude times the soft factor:

$$\mathcal{M}^\mu(\{p_i\}, q) \simeq \mathcal{M}_0(\{p_i\}) \sum_{i=1}^{N} \frac{e_i \eta_i p_i^\mu}{p_i \cdot q - i\eta_i \varepsilon} \tag{1.4.4}$$

In order to compute the scattering amplitude one then has to contract $\mathcal{M}^\mu$ with the photon's "wave function" and integrate over its 4-momentum. As already discussed, the factorized form of Eq. (1.4.4) will still hold at the cross section level only if the phase space factorizes accordingly.

A couple of remarks are due before proceeding to the QCD counterpart of the factorization theorem:

- Since a soft photon emitted during a scattering process can't be detected by any experimental piece of equipment, when computing any scattering amplitude

  $$p_1 + p_2 + ... + p_m \longrightarrow p_{m+1} + p_{m+2} + ... + p_n \tag{1.4.5}$$

  one also has to include in the calculation all of the related processes where one or more photons of soft momenta $k_1, k_2, ...k_r$ are emitted:

  $$p_1 + ... + p_m \longrightarrow p_{m+1} + ... + p_n + k_1 + ... + k_r \tag{1.4.6}$$

  This justifies the need to consider multiple soft photon emissions, never mind how inclusive one's cross section is. On the other hand a collinear, hard photon changes the final state in a way that is measurable, therefore it should not be included in the computation of $\mathcal{M}$.

- The classification of the various soft emissions tacitly assumed that only the hard external lines could emit soft photons, while other already emitted soft photons could not do so. This is true in QED (and gravity) since the photon does not carry any electric charge, but will not be true in non-abelian Yang-Mills theories such as QCD where the gauge bosons, the gluons, do carry a color charge.

As a result, the soft emissions of QCD become more and more convoluted as one tries to include correlations between various emission. Nevertheless, a factorized form of a generic QCD matrix element is known un to NNLL precision [8].

1.4.2 QCD Matrix element factorization

We can now derive a factorized form of a QCD matrix element when soft and collinear gluon emissions occur. Because of the confined nature of QCD, a gluon collinear to final state (colored) momentum p will not be detectable in an experimental setting. Indeed, it will be impossible to distinguish it from the gluons present in the hadron associated to the momentum p after the hadronization process.

Since we have to include real collinear gluon emissions in our calculation, we can no longer rely solely on the soft factorization theorem as we did in QED since a collinear gluon is generally not soft. Nevertheless the matrix element can be factorized in a universal fashion; in this Section we prove factorization of the matrix element with respect to the emission of one gluon, the generalization to multiple gluon emissions is straightforward[1].

Consider a process initiated by two quarks of momenta:

$$p_1^\mu = \frac{\sqrt{s}}{2}(1,0,0,1), \qquad p_2^\mu = \frac{\sqrt{s}}{2}(1,0,0,-1), \tag{1.4.7}$$

then suppose one of the particles, say p_1, radiates a gluon of momentum q. The matrix element for this process is:

$$i\mathcal{M}(p_1,p_2) = i\sqrt{\alpha_s}\mathcal{M}(p_1-q,p_2)\frac{\not{p}_1-\not{q}}{(p_1-q)^2}\gamma^\mu t^a u(p_1)\varepsilon_\mu(q) \tag{1.4.8}$$

where $\mathcal{M}(p_1-q,p_2)$ is the Born level matrix element with the correct incoming momenta, $\varepsilon_\mu(q)$ is the gluon's polarization vector and $u(p_1)$ is the polarization vector of the first quark.

We parametrize the 4-momentum q in terms of the incoming momenta and a transverse spacelike momentum $q_\perp$:

$$q = (1-z)p_1 + q_\perp + \xi p_2 \tag{1.4.9}$$

[1] This is only true if uncorrelated gluon emissions are considered. The proof of matrix element becomes more convoluted when one also considers emissions from other emitted soft and/or collinear gluon. Luckily these can be classified in a hierarchy: at LL accuracy one only need to consider uncorrelated emissions, at NLL one has to include two-particles correlations and so on. More details can be found in Ref.[13].

The on-shell condition for the gluon fixes:

$$\xi = \frac{q_\perp^2}{2(p_1 \cdot p_2)(1-z)} \tag{1.4.10}$$

Substituting in Eq.(1.4.8) and retaining only the most singular terms in $q_\perp$ we get:

$$i\mathcal{M}(p_1, p_2) = i\sqrt{\alpha_s}\mathcal{M}(p_1 - q, p_2)\frac{(1-z)(\not{p}_1 - \not{q})}{-q_\perp^2}\gamma^\mu t^a u(p_1)\varepsilon_\mu(q) \tag{1.4.11}$$

We then rewrite the momentum p_1 as:

$$p_1 = \frac{q - q_\perp - \xi p_2}{(1-z)} \tag{1.4.12}$$

and, after some algebra, using the Dirac equation for $u(p_1)$ and $\{\not{q}_\perp, \gamma^\mu\} = 2q_\perp^\mu$ we obtain for the matrix element:

$$i\mathcal{M}(p_1, p_2) = i\sqrt{\alpha_s}\mathcal{M}(p_1 - q, p_2)\frac{-2zq_\perp^\mu - (1-z)\not{q}_\perp\gamma^\mu}{-q_\perp^2}\gamma^\mu t^a u(p_1)\varepsilon_\mu(q) \tag{1.4.13}$$

Taking the square modulus of the amplitude and summing over polarizations we get:

$$|\mathcal{M}(p_1, p_2)|^2 = \alpha_s C_F \frac{(1+z^2)}{q_\perp^2}|\mathcal{M}_B|^2 \tag{1.4.14}$$

Where:

$$|\mathcal{M}_B|^2 = \sum |u(p_1 - q)\mathcal{M}(p_1 - q, p_2)|^2 \tag{1.4.15}$$

Therefore we see that the emission of a soft and/or collinear gluons from a quark contributes to the matrix element squared with a factor:

$$\alpha_s C_F \frac{(1+z^2)}{q_\perp^2} \tag{1.4.16}$$

In general the soft/collinear emission of a colored particle brings a factor:

$$\alpha_s \frac{p_{ij}(z)}{q_\perp^2} \tag{1.4.17}$$

where p_{ij} is the numerator of the Atarelli-Parisi splitting function.

This result can be straightforwardly extended to the emission of multiple gluons as long as one does not consider correlations between different emissions. Including these corrections is actually needed to perform the resummation at the NNLL accuracy and further; a complete discussion can be found in Ref.[13].

1.4.3 Phase space factorization

In order to proceed with the resummation program one has to multiply the matrix element with the phase space and integrate over the radiation's degrees of freedom. If the cross section obtained this way can be written in a factorized form, one is able to exponentiate the soft/collinear contributions as will be discussed in the next section.

In the case of threshold resummation the phase space for the emission of m gluons with momentum fractions $z_1, z_2, ..., z_m$ from an incoming/outgoing leg will be proportional to[1]:

$$dz_1 \cdots dz_m \delta(z - z_1 \cdots z_n) \tag{1.4.18}$$

which clearly does not factorize. The Dirac delta can be brought into a factorized form taking the Mellin transform of the cross section, indeed:

$$\begin{aligned} \mathcal{M}\left[\delta(z - z_1 \cdots z_n)\right](N) =& \int_0^1 \frac{dz}{z} \delta(z - z_1 \cdots z_n) \\ =& z_1^{N-1} \cdots z_m^{N-1} \end{aligned} \tag{1.4.19}$$

Then the z_i integration included in the $i-$th gluon's phase space integration became, thanks to the z^{N-1} terms in (1.4.19), a Mellin transform with respect to z_i.

This is a simple argument showing that in general threshold factorization (and thus threshold resummation) has to be performed in Mellin space. The factorization of the phase space is not trivial by any means and I will not discuss further the issues related to it since they have been discussed heavily in the literature[7, 8, 20].

The most important feature of the soft/collinear factors is that they are logarithmically enhanced. This shows that the origin of the large logarithms that spoil the perturbative expansion can be traced back to the emission of soft and collinear gluons, as we had already anticipated.

1.5 Large logarithms - the Resummation

Once the factorization of the large logarithmic terms has been properly accomplished, one can proceed with their exponentiation, which concludes the

[1] The Dirac delta comes from the longitudinal component of the 4-momentum conservation law.

resummation procedure.

Suppose that the emission of a single gluon amounts to a factor:

$$\int d^3q\sigma(\{p_i\}, q) = \sigma(\{p_i\})\mathcal{S}(\alpha_s \ln N, \alpha_s) \tag{1.5.1}$$

where I will call S the Sudakov form factor for historic reasons and I am implicitly assuming that the cross sections are considered in the Mellin space where factorization occurs. The Sudakov form factor has a logarithmic expansion:

$$\mathcal{S}(\lambda, \alpha_s) = \frac{1}{\alpha_s} g_1(\lambda) + g_2(\lambda) + \alpha_s g_3(\lambda) + ... \tag{1.5.2}$$

Since we assume complete factorization holds at the cross section level the emission of M gluons amounts to:

$$\int \prod d^3q_j \sigma(\{p_i\}, \{q_j\}) = \frac{1}{M!}\sigma(\{p_i\}) \prod \mathcal{S}(\alpha_s, x) \tag{1.5.3}$$

Where the $1/M!$ is the combinatorics factor for M bosons. Summing over all possible M we get a power series in S which can be written as an exponential:

$$\sigma^{rad}(\{p_i\}) = \sigma(\{p_i\}) g_0(\alpha_s) \exp\{\mathcal{S}(\alpha_s, x)\} \tag{1.5.4}$$

The cross section σ^{rad} contains the soft and collinear contributions from every possible number of gluon emission. The function g_0 takes into account the virtual contributions and can be computed as a power expansion in α_s. The resummed cross section can be computed perturbatively by truncating the expansion (1.5.2). This expansion, however, is different from the fixed order one, indeed by including the function g_1 we are actually including a complete tower of logarithms, namely all the terms:

$$\ln N^{2n} \alpha_s^n \tag{1.5.5}$$

Including those terms (for every n) together with the 0-th order of g_0 correspond to a *leading logarithm* (LL) computation.

Correspondingly, including all the g functions up to g_{k+1} together with g_0 computed up to order α_s^k will result in a N^{k}LL computation, and will properly resum all the $\ln N^{2n-j}\alpha_s^n$ terms with $j \leq k$.

A quick remark about the process of exponentiation: since in general $\mathcal{S}$ will be a matrix in color space, the exponential will be well defined only with a proper path ordering.

	LO	NLO	NNLO	$\cdots$
LL	-	$\alpha_s \ln^2$	$\alpha_s^2 \ln^4$	...
NLL	-	$\alpha_s \ln$	$\alpha_s^2 \ln^3$	...
NNLL	-	α_s	$\alpha_s^2 \ln^2$	...
$\cdots$	-	-	...	...

Table 1.2: *Logarithmic towers in fixed order and resummed accuracy.*

1.6 Threshold resummation in $p_\perp$-spectrum for Higgs production

In this section I will present the results for the threshold resummation at fixed $p_\perp$ for the transverse momentum distribution in Higgs production. This was developed at NLL accuracy in Refs. [6, 7] for every partonic channel: we are interested in the gluon fusion channel and therefore we will only present the results for the particular subprocess:

$$g_1 + g_2 \longrightarrow H + X \tag{1.6.1}$$

The resummed $p_\perp$ distribution can be written as:

$$\frac{d\sigma_{gg}^{res}}{dp_\perp^2} = \frac{d\sigma_{gg}^{LO}}{dp_\perp^2} g_{0,gg}(p_\perp^2) \exp[\mathcal{G}(N, p_\perp^2)] \tag{1.6.2}$$

with

$$\mathcal{G}(N, p_\perp^2) = \Delta_g(N) + \Delta_g(N) + J_g(N) + \Delta_{int}(N, p_\perp^2) \tag{1.6.3}$$

The Sudakov exponent $\mathcal{G}$ gets contributions from gluon radiation off the incoming gluons (the Δ terms), the outgoing gluon (the J term) and from an interference term related to large-angle emission (the Δ_{int} term). In particular, the only $p_\perp$ dependence in the Sudakov exponent is the one coming from the interference term Δ_{int}.

From now on we will drop the partonic subscript since we will only investigate the gluon fusion channel where both the incoming partons and the LO radiation are gluons[1].

The various contributions to the Sudakov exponent (1.6.3) are defined as[2]:

[1]Moreover there is only one possible color structure, rendering the Sudakov exponent diagonal in color space and making the exponentiation in (1.6.2) a simple exponential function.

[2]We change a sign in the Δ_{int} term found in Ref. [8], Eq. (2.3.5) since it does not match with the original paper where the result was firstly derived[6]. We have checked

$$\Delta(N) = \int_0^1 dz \frac{z^{N-1}-1}{1-z} \int_{\mu_F^2}^{\tilde{Q}^2(1-z)^2} \frac{dq^2}{q^2} A(\alpha_s(q^2)) \tag{1.6.4}$$

$$J(N) = \int_0^1 dz \frac{z^{N-1}-1}{1-z} \int_{\tilde{Q}^2(1-z)^2}^{\tilde{Q}^2(1-z)} \frac{dq^2}{q^2} A(\alpha_s(q^2)) + B\left(\alpha_s\left(\tilde{Q}^2(1-z)\right)\right) \tag{1.6.5}$$

$$\Delta_{int}(N, p_\perp^2) = \int_0^1 dz \frac{z^{N-1}-1}{1-z} A\left(\alpha_s\left(\tilde{Q}^2(1-z)^2\right)\right) \ln \frac{(\sqrt{1+\xi}+\sqrt{\xi})^2}{\xi} \tag{1.6.6}$$

where $\xi = p_\perp^2/m^2$ is an adimensional variable for the transverse momentum, $\tilde{Q}^2 = Q^2(\sqrt{1+\xi}+\sqrt{\xi})^2$ is the relevant hard scale of the process and $A(\alpha_s)$, $B(\alpha_s)$ can be computed as power series in α_s:

$$A(\alpha_s) = A_g(\alpha_s) = A^{(1)}\alpha_s + A^{(2)}\alpha_s^2 + \mathcal{O}(\alpha_s^4) \tag{1.6.7}$$

$$A^{(1)} = \frac{C_A}{\pi} \tag{1.6.8}$$

$$A^{(2)} = \frac{C_A}{2\pi^2}\left[C_A\left(\frac{67}{18} - \zeta_2\right) - \frac{5}{9}n_f\right] \tag{1.6.9}$$

$$B(\alpha_s) = B_g(\alpha_s) = B^{(1)}\alpha_s + \mathcal{O}(\alpha_s^4) \tag{1.6.10}$$

$$B^{(1)} = -\beta_0 = -\frac{11C_A + 2n_f}{12\pi} \tag{1.6.11}$$

These coefficients enable us to compute the resummed cross section up to NLO accuracy: the interested reader may find the explicit expressions for the g_1 and g_2 functions in Ref. [6].

We will rather compute explicitly the fixed order expansion of the resummed cross section:

$$\frac{d\sigma^{res}}{d\xi} = \left.\frac{d\sigma^{res}}{d\xi}\right|_{LO} + \left.\frac{d\sigma^{res}}{d\xi}\right|_{NLO} + ... \tag{1.6.12}$$

The LO term is simply:

$$\left.\frac{d\sigma^{res}}{d\xi}\right|_{LO} = \frac{d\sigma^{LO}}{d\xi} \tag{1.6.13}$$

In order to compute the NLO term one has to compute the exponential in Eq.(1.6.2) up to $\mathcal{O}(\alpha_s)$ and the function g_0 up to the same order. We

that the definitions of the Sudakov exponent in the two papers match by setting $\mu_F^2 = m^2\tilde{a}$ provided one changes the sign of the Δ_{int} term.

will not bother to compute the contributions coming from the g_0 functions, since they are not logarithmically enhanced in the large N region[1].

The power series for the Sudakov form factor and the corresponding series for its exponential are, up to $\mathcal{O}(\alpha_s)$:

$$\mathcal{G}(N,\xi) = \alpha_s \mathcal{G}^{(1)}(N,\xi) + \mathcal{O}(\alpha_s^2) \tag{1.6.14}$$

$$\exp\left[\mathcal{G}(N,\xi)\right] = 1 + \alpha_s \mathcal{G}^{(1)}(N,\xi) + \mathcal{O}(\alpha_s^2) \tag{1.6.15}$$

There are two ways of computing the functions $\mathcal{G}^{(k)}$. One can compute them from the logarithmic expansion of $\mathcal{G}$, analogous to the one presented for the general case Eq.(1.5.2), by expanding the g_i functions to fixed order. Then from the NLL resummed cross section that includes the g_1 and g_2 functions one is able to compute the single and double logarithmic behavior of $\mathcal{G}^{(1)}$, while in order to compute the constant term one also needs to know the g_3 function (which is included in the NNLL cross section).

We will not adopt this method, although we have checked that the results obtained in this way match the ones we are about to present. We are rather going to compute the Sudakov terms Eqs. (1.6.4)-(1.6.6) at fixed order accuracy:

$$\mathcal{G}^{(1)}(N,\xi) = 2\Delta^{(1)}(N) + J^{(1)}(N) + \Delta^{(1)}_{int}(N,\xi) \tag{1.6.16}$$

where the terms on the right hand side are obviously the coefficients of the corresponding Sudakov terms in a fixed order expansion. For the sake of briefness we will compute $J^{(1)}$ explicitly and will only give the final result for the other two coefficients, since their computations is very similar.

Expanding A up to first order in (1.6.4) we get:

$$\begin{aligned} J^{(1)}(N) &= \int_0^1 dz \frac{z^{N-1}-1}{1-z} \int_{\tilde{Q}^2(1-z)^2}^{\tilde{Q}^2(1-z)} \frac{dq^2}{q^2} A^{(1)} + B^{(1)} \\ &= \int_0^1 dz \frac{z^{N-1}-1}{1-z} \left(-A^{(1)} \ln(1-z) + B^{(1)}\right) \end{aligned} \tag{1.6.17}$$

The z integrations can be thought of as special cases of the integral:

$$\int_0^1 dz \left(\frac{\ln^k(1-z)}{1-z}\right)_+ z^{N-1} \tag{1.6.18}$$

[1]The interested reader will find the expression for g_0 up to $\mathcal{O}(\alpha_s)$ in Ref.[8], Appendix C.

Where the plus distribution is defined as in Appendix A. These integrals can be solved for all k from a generating integral in a systematic way[1]. The specific results we are going to need are:

$$\int_0^1 dz \left(\frac{1}{1-z}\right)_+ z^{N-1} = -\psi_0(N) - \gamma_E \tag{1.6.19}$$

$$\int_0^1 dz \left(\frac{\ln(1-z)}{1-z}\right)_+ z^{N-1} = \frac{1}{2}\left[\psi_0^2(N) - \psi_1(N) + 2\gamma_E\psi_0(N) + \zeta_2 + \gamma_E^2\right] \tag{1.6.20}$$

where ψ are Poligamma functions, γ_E is Euler's constant and $\zeta_2 = \zeta(2)$ is Riemann's zeta function evaluated at $2+0i$. Therefore the J term is:

$$\begin{aligned} J^{(1)}(N) = &-\frac{A^{(1)}}{2}\left[\psi_0^2(N) - \psi_1(N) + 2\gamma_E\psi_0(N) + \zeta_2 + \gamma_E^2\right] \\ &+ B^{(1)}\left[-\psi_0(N) + \psi_0(1)\right] \end{aligned} \tag{1.6.21}$$

In the large N limit, where the resummed cross section gives reliable informations, it amounts to:

$$J^{(1)}(N) = -\frac{A^{(1)}}{2}\left[\ln^2 N + 2\gamma_E \ln N + \zeta_2 + \gamma_E^2\right] - B^{(1)}\left[\ln N + \gamma_E\right] \tag{1.6.22}$$

where we used the asymptotic behavior of the Poligamma functions, namely $\psi_0(N) \sim \ln N$ and $\psi_i(N) \to 0$ for $i \geq 1$ in the large N region.

After computing the remaining terms in the Sudakov exponent one obtains for the resummed cross section expanded at NLO:

$$\begin{aligned} &\left.\frac{d\sigma^{res}}{d\xi}\right|_{NLO}(N,\xi) = \\ &\quad \frac{d\sigma^{LO}}{d\xi}(N,\xi)\frac{\alpha_s}{2\pi}\left\{c_2 \ln^2 N + c_1(\xi)\ln N + c_0(\xi) + \mathcal{O}\left(\frac{1}{N}\right)\right\} \end{aligned} \tag{1.6.23}$$

Where[2]:

$$c_2 = 3C_A \tag{1.6.24}$$

$$c_1(\xi) = 6C_A\gamma_E + 2\pi\beta_0 - C_A \ln\frac{\tilde{a}}{\xi} - 2C_A \ln\frac{Q^2}{\mu_F^2} \tag{1.6.25}$$

$$c_0(\xi) = 3C_A(\zeta_2 + \gamma_E^2) + 2\pi\beta_0\gamma_E - C_A\gamma_E \ln\frac{\tilde{a}}{\xi} - 2C_A\gamma_E \ln\frac{Q^2}{\mu_F^2} \tag{1.6.26}$$

[1] The computation of these and other integrals involving plus distributions can be found in Ref.[9].

where $\tilde{a} = \tilde{a}(\xi) = (\sqrt{1+\xi} + \sqrt{\xi})^2$.

[2] We remind the reader that we are still using conventions where $\beta_0 = \frac{11C_A - 2n_f}{12\pi}$.

Chapter 2

Higgs boson inclusive production beyond NNLO

This chapter is the review of an article from Ball, Bonvini, Forte, Marzani and Ridolfi[1]. The article proposes an approximation for the N^{3}LO inclusive cross section for Higgs production via gluon fusion in p-p collisions.

This thesis aims to extend the results found in this article for the inclusive cross section to the semi-differential one, namely the $p_\perp$ distribution. This task will be tackled in Chapter 4 but the main concepts that lead to this result are already there in the simpler case of the inclusive cross section reviewed in this Chapter.

The approximation is achieved by exploiting the all-order threshold informations contained in the resummed cross section and the known analytic structure of the fixed order cross section in Mellin space. It is argued that the resummed cross section is unreliable far away from threshold (in the large N region) largely because it does not have the correct singularity structure. Loosely speaking, the large logarithms that appear in the resummed cross section when expanded at fixed order have cut singularities in the N complex plane, while the fixed order cross section has pole singularities.

By backtracking the origin of those large logarithms, one is able to find the functions that generates them in the $N \to \infty$ limit. This function has to have the correct pole structure while still be unambiguously paired with a threshold logarithm[1]. One can then substitute this function in place of the $\ln(N)$ in the resummed cross section obtaining the desired approximation.

[1]Since our approximation is technically a prescription for including terms that are subleading in the threshold region, this last statement could be rephrased as "We need to keep only subleading terms that we know will appear with every corresponding logarithm

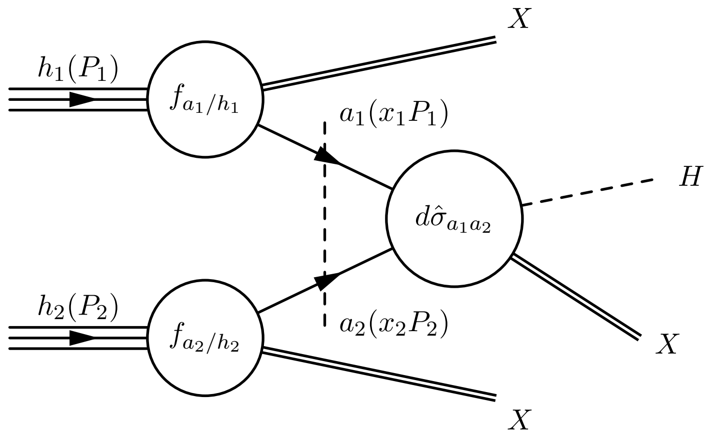

Figure 2.1: *Factorization theorem for the production of an Higgs particle. The vertical dashed line separates the low energy, non-perturbative dynamic on the left from the high energy partonic cross section in the right.*

Throughout this chapter I will adopt the same notation as Ref.[1], may the reader be aware that the variables definitions contained in this chapter do not necessarily hold in the remaining of this body of work.

2.1 Large logarithms in Mellin space

Consider the production of an Higgs boson in a p-p collision schematically represented in Fig.2.1.

The cross section for this process, thanks to the factorization theorem, can be written as:

$$\sigma(\tau, m^2) = \tau \sum_{ij} \int_\tau^1 \frac{dz}{z} \mathcal{L}_{ij}(\frac{\tau}{z}, \mu_F^2) \frac{1}{z} \hat{\sigma}_{ij} \left(z, m^2, \alpha_s(\mu_R^2), \frac{m^2}{\mu_F^2}, \frac{m^2}{\mu_R^2} \right) \quad (2.1.1)$$

where $\tau \equiv m^2/s$ and $\mathcal{L}_{ij}$ are the parton luminosities.

We define the coefficient functions C as:

$$\hat{\sigma}_{ij} \left(z, m^2, \alpha_s(\mu_R^2), \frac{m^2}{\mu_F^2}, \frac{m^2}{\mu_R^2} \right) = z\sigma_0(m^2, \alpha_s(\mu_R^2)) C_{ij} \left(z, \alpha_s(\mu_R^2), \frac{m^2}{\mu_F^2}, \frac{m^2}{\mu_R^2} \right) \quad (2.1.2)$$

while still keeping enough subleading terms in order to preserve the original fixed order cross section.".

and normalize the parton luminosities in order for the 0-th order gg coefficient function to be a Dirac delta:

$$C_{ij}(z,\alpha_s) = \delta(1-z)\delta_{ig}\delta_{jg} + \alpha_s C_{ij}^{(1)}(z) + \alpha_s^2 C_{ij}^{(2)}(z) + \alpha_s^3 C_{ij}^{(3)}(z) + \mathcal{O}(\alpha_s^4) \tag{2.1.3}$$

2.1.1 NLO fixed order cross section

We only consider the gluon fusion channel, therefore setting $i,j=g$ in all our equations and dropping the corresponding labels from now on.

The $\mathcal{O}(\alpha_s)$ coefficient is given by[13, 8]:

$$C^{(1)}(z) = 4A_g(z)\mathcal{D}_1(z) + d\delta(1-z) - 2A_g(z)\frac{\ln z}{1-z} + \mathcal{R}_{gg}(z), \tag{2.1.4}$$

$$\mathcal{D}_k(z) \equiv \left(\frac{\ln^k(1-z)}{1-z}\right)_+ , \tag{2.1.5}$$

$$A_g(z) \equiv \frac{C_A}{\pi}\frac{1-2z+3z^2-2z^3+z^4}{z} \tag{2.1.6}$$

Where R is a regular function of z in $z=1$ and both R and d depend on m/m_t.

The threshold region corresponds in Mellin space to the $N\to\infty$ limit. Therefore in order to study the threshold behavior of the NLO cross section we are only interested in those terms that give contribution al large N. Since the Mellin transform of an ordinary function vanished as $N\to\infty$[9] the last two terms in (2.1.4) do not contribute to the threshold limit. The delta term is constant in Mellin space while the $\mathcal{D}_1$ term is divergent as $N\to\infty$. Indeed[9]:

$$\begin{aligned} \mathcal{D}_1(N) \equiv& \int_0^1 x^{N-1}\mathcal{D}_1(x)dx \\ =&\frac{1}{2}[\psi_0^2(N) - \psi_1(N) + 2\gamma_E\psi_0(N) + \zeta_2 + \gamma_E^2] \end{aligned} \tag{2.1.7}$$

$$\mathcal{D}_1(N) \xrightarrow{N\to\infty} \frac{1}{2}[\ln^2(N) + 2\gamma_E\ln(N) + \zeta_2 + \gamma_E^2] \tag{2.1.8}$$

We can already see that in this last limit we are modifying the singularity structure, loosing the correct pole structure in favor of branch cuts. This can be rephrased as saying that we are discarding some subleading terms which do not change the threshold limit but greatly affect the low N region.

The objective is then to find a prescription for retrieving systematically those terms, or roughly speaking to "invert" the approximation made in Eq.(2.1.8).

2.1.2 Resummed cross section

The contributions to the coefficient function that do not vanish in the threshold limit can be computed at all orders from the resummed cross section.

The resummed coefficient function can be written as:

$$C_{res}(N,\alpha_s) = g_0(\alpha_s)\exp\left[\frac{1}{\alpha_s}g_1(\alpha_s\ln N) + g_2(\alpha_s\ln N) + \alpha_s g_3(\alpha_s\ln N) + ...\right] \tag{2.1.9}$$

When expanded at any fixed order it gives the logarithmically enhanced and constant terms in the threshold limit. Expanding C_{res} up to $\mathcal{O}(\alpha_s)$ we get:

$$C_{res}(N,\alpha_s) = 1 + \alpha_s C^{(1)}_{res}(N) + \mathcal{O}(\alpha_s^2), \tag{2.1.10}$$

$$C^{(1)}_{res}(N) = \frac{2C_A}{\pi}[\ln^2 N + 2\gamma_E\ln N + g_{0,1}] \tag{2.1.11}$$

As expected, the large N behavior of the fixed order and resummed coefficient are the same[1]:

$$\lim_{N\to\infty}\left[C^{(1)}_{res}(N) - C^{(1)}(N)\right] = 0 \tag{2.1.12}$$

While the large N behavior is the same, the two coefficients $C^{(1)}$ and $C^{(1)}_{res}$ differ greatly in the low N region. Indeed the resummed result is expected to be reliable only in the threshold limit.

More precisely, the fixed coefficient has pole singularities given by the Poligamma functions while the resummed one has cut singularities given by the $\ln N$. While both these singularities do lie outside the physical region $N > 0$ they are close enough to it to produce wildly different results for the cross section at low N.

In the low N region the fixed order cross section is not affected by large kinematic terms and is therefore reliable. We can thus say that the correct singularity structure to be had is the one given by $C^{(1)}$ while the cuts exhibited by the resummed coefficients are artifacts of the resummation procedure.

[1] The logarithmic behavior is correcly predicted from general arguments while the constant $g_{0,1}$ is fixed by requiring Eq.(2.1.12) to hold

If we were to know the resummed coefficient but not the fixed order one, and wanted to make an approximation to the former we would do a much better job by substituting the $\ln N$ with Poligamma functions.

2.2 Refined approximation

The approximation we just proposed is justified by backtracking the kinematical origin of the large logarithms. Indeed, just from comparing the fixed order and resummed coefficients at NLO we did't obtain informations about the structure of the threshold logarithms at higher orders, although it enabled us to make an educated guess.

The large threshold logarithms originate from the integration of real emission diagrams over the emitted gluon's transverse momentum:

$$p_{gg}(z)\int_{\Lambda}^{\frac{M(1-z)}{\sqrt{z}}}\frac{dk_{\perp}}{k_{\perp}}=\frac{A_g(z)}{1-z}\left(\ln\frac{1-z}{\sqrt{z}}+\ln\frac{M}{\Lambda}\right) \tag{2.2.1}$$

where Λ is a collinear cutoff and:

$$p_{gg}(z)=\frac{A_g(z)}{1-z} \tag{2.2.2}$$

Therefore the logarithmically enhanced terms at all orders are of the form:

$$\frac{1}{1-z}\ln\frac{1-z}{\sqrt{z}}=\frac{1}{1-z}\left[\ln(1-z)+\mathcal{O}(1-z)\right] \tag{2.2.3}$$

This not only justifies the approximation proposed in the previous section, but also suggests a more refined one. Namely, instead of identifying solely the $\mathcal{D}_1$ function as the origin of the large logarithms we can instead take:

$$\hat{\mathcal{D}}_1(z)\equiv\left(\frac{\ln(1-z)}{1-z}\right)_+-\frac{\ln\sqrt{z}}{1-z} \tag{2.2.4}$$

or more precisely its Mellin transform to be the proper substitute for the $\ln N$ terms.

Both $\hat{\mathcal{D}}_1$ and $\mathcal{D}_1$ correctly reproduce the large N behavior[1]and have a pole singularity structure, yet the former reproduces the double poles in $N=0,-1,-2,...$ that are present in the fixed order result while the latter only has single poles.

[1]For the constant term matching, we redirect the interested reader to the original article[1], especially the first appedix.

In summary the approximation is constructed in the following way. The resummed coefficient is rewritten as:

$$C_{res}(N,\alpha_s) = g_0(\alpha_s)\exp\sum_{n=1}^{\infty}\alpha_s^n\sum_{k=0}^{n} b_{n,k}\mathcal{D}_k^{log}(N) \tag{2.2.5}$$

Where:

$$\mathcal{D}_k^{log}(z) \equiv \left(\frac{\ln^k \ln\frac{1}{z}}{\ln\frac{1}{z}}\right)_+, \qquad \mathcal{D}_k^{log}(N) \equiv \mathcal{M}\left[\mathcal{D}_k^{log}(z)\right](N) \tag{2.2.6}$$

and $M[f]$ is the Mellin transform of any function f.

Then one of two substitutions is done[1], resulting in:

$$C_{soft1}(N,\alpha_s) = \bar{g}_0(\alpha_s)\exp\sum_{n=1}^{\infty}\alpha_s^n\sum_{k=0}^{n} b_{n,k}\hat{\mathcal{D}}_k(N+1) \tag{2.2.7}$$

$$\begin{aligned} C_{soft2}(N,\alpha_s) = &\bar{g}_0(\alpha_s)\exp\sum_{n=1}^{\infty}\alpha_s^n\sum_{k=0}^{n} b_{n,k}\times \\ &\times\left[2\hat{\mathcal{D}}_k(N) - 3\hat{\mathcal{D}}_k(N+1) + 2\hat{\mathcal{D}}_k(N+2)\right] \end{aligned} \tag{2.2.8}$$

Equations (2.2.7)-(2.2.8) give the desired approximation for the NNLO fixed order inclusive cross section satisfying all of the properties required: they correctly reproduce the threshold logarithmic behavior while still exhibiting the desired pole structure; moreover they can be computed solely from the resummed cross section.

Since the NNLO fixed order cross section is known[15, 16, 5], it is possible to check numerically the goodness of the approximation. The interested reader may find this comparison in the original paper[1].

[1] The two approximations soft1 and soft2 differ in that the former takes into account the threshold expansion of $A_g(z)$ up to second order while the latter up to first order[1].

Chapter 3

Higgs $p_\perp$-spectrum at NLO

In order to adopt a similar strategy to the one presented in Ref.[1][1]in the context of $p_\perp$ distributions we need to compare the logarithmic terms arising in the fixed order computation to the ones predicted by resummation theory.

The lowest perturbative order in which this comparison is possible is the NLO order[2], since it is the first order where real, soft gluon emissions do contribute to the $p_\perp$-spectrum.

Unfortunately, the NLO $p_\perp$ distribution for Higgs production via gluon fusion is only available in literature in numerical form. Since we are interested in the precise form of the logarithmic terms and their singularity structure we will need to derive the analytic form of the NLO $p_\perp$-spectrum first, at least in the threshold limit.

The closest result available in analytic form in the literature to the one we are interested in is the double differential cross section in rapidity y and transverse momentum $p_\perp$. This distribution was computed by Glosser up to NLO[3] using elicity techniques, the final results were presented by Glosser and Schmidt[4].

This Chapter will be devoted to the rapidity integration of the result from Glosser regarding the gluon fusion channel. The techniques used during the computation are applicable also to the other partonic channels; we leave this exercise to future researchers.

---

[1]We quickly reviewed the content of this article in Chapter 2, the interested reader may find more informations in the original paper.

[2]We remind the reader of the different “order terminology” used in inclusive and differential cross sections explained in Sec.1.2.1.

3.1 Notation and Mandelstam variables

As already stated before we will consider the process:

$$h_1(P_1) + h_2(P_2) \to H(p) + X(Q) \tag{3.1.1}$$

where h_i are the incoming hadrons, H is the Higgs boson we are interested in and X is any extra radiation.

The corresponding partonic process in the gluon fusion channel is:

$$g_1(p_1) + g_2(p_2) \to H(p) + X(Q) \tag{3.1.2}$$

We parametrize the momenta in the partonic center of mass frame:

$$\begin{aligned} p_1 &= \frac{\sqrt{s}}{2}(1,0,0,1), & p_2 &= \frac{\sqrt{s}}{2}(1,0,0,-1), \\ p &= (E_H, \overrightarrow{p_\perp}, p_L), & Q &= (Q_0, -\overrightarrow{p_\perp}, -p_L) \end{aligned} \tag{3.1.3}$$

The rapidity along the z axis of the Higgs boson is defined as:

$$y \equiv \ln \frac{E_H + p_L}{m_\perp}, \qquad m_\perp^2 = m^2 + p_\perp^2 \tag{3.1.4}$$

where m is the mass of the Higgs boson and $m_\perp$ is called the transverse mass. In terms of the rapidity and the transverse mass the Higgs' boson momentum can be written as:

$$p = (m_\perp \cosh(y), \overrightarrow{p_\perp}, m_\perp \sinh(y)) \tag{3.1.5}$$

We stress that, even if all of the radiation is made up of massless particles, the 4-momentum Q is the sum of all the radiated particles' momenta and therefore in general:

$$Q^2 \geq 0 \tag{3.1.6}$$

and the equality holds if all the radiation is either soft or collinear to the Higgs momentum.

The partonic Mandelstam variables are defined as:

$$s \equiv (p_1 + p_2)^2, \qquad t \equiv (p_1 - p)^2, \qquad u \equiv (p_1 - Q)^2 \tag{3.1.7}$$

i.e. by considering all the radiation Q as a single particle; they are well defined for any number of radiated gluons.

In terms of the rapidity and the transverse momentum these can be written as:

$$t = m^2 - m_\perp^2 e^{-y}, \tag{3.1.8}$$
$$u = m^2 - m_\perp^2 e^{y}, \tag{3.1.9}$$

Energy momentum conservation at the partonic level implies:

$$s + t + u = \sum m_i^2 = m^2 + Q^2 \tag{3.1.10}$$

Therefore we can write Q^2 as a function of y and $p_\perp$:

$$Q^2 = s + t + u - m^2 = s + m^2 - m_\perp \sqrt{s}\left(e^y + e^{-y}\right) \tag{3.1.11}$$

In accordance to the literature[8] we define:

$$\begin{aligned} \tau =& \frac{m^2}{s}, \qquad & 0 \leqslant \tau \leqslant a(\xi) \\ \xi =& \frac{p_\perp^2}{m^2}, \qquad & 0 \leqslant \xi \leqslant \frac{(1-\tau)^2}{4\tau} \end{aligned} \tag{3.1.12}$$

Where either of the kinetically allowed range is considered at fixed value of the other variable. As we can see from Eq.(3.1.12) the variable τ, which was identified as the threshold variable in the inclusive case, does not range from 0 to 1 but rather is bounded from above by[8]:

$$a(\xi) \equiv (\sqrt{\xi - 1} - \sqrt{\xi})^2 \tag{3.1.13}$$

It is convenient to define a threshold variable that ranges from 0 to 1, and more importantly whose range does not depend of $p_\perp$ (or equivalently on ξ):

$$x \equiv \frac{\tau}{a(\xi)} = \frac{m^2}{s}(\sqrt{\xi - 1} + \sqrt{\xi})^2 \tag{3.1.14}$$

With respect to the variables x and ξ the physical region is:

$$0 \leqslant x \leqslant 1, \qquad 0 \leqslant \xi \tag{3.1.15}$$

Finally, for future convenience we define:

$$\tilde{a}(\xi) \equiv (\sqrt{\xi - 1} + \sqrt{\xi})^2 = \frac{1}{a(\xi)} \tag{3.1.16}$$

3.2 $p_\perp$ and y differential distribution up to NLO

The factorization theorem for the double differential cross section states that the hadronic cross section can be written as:

$$\frac{d\sigma}{dp_T^2 dy} = \sum_{i,j} \int_0^1 dx_1 dx_2 f_{i,h_1}(x_1, \mu_F) f_{j,h_2}(x_2, \mu_F) \frac{d\hat{\sigma}_{ij}}{dp_T^2 dy} \tag{3.2.1}$$

where f are the parton distribution functions (PDF) and $d\hat{\sigma}/dp_T^2 dy$ is the partonic differential cross section.

The partonic cross section admits the perturbative expansion[1]:

$$\frac{d\hat{\sigma}_{ij}}{dp_T^2 dy} = \frac{\sigma_0}{s} \left[\frac{\alpha_s(\mu_R)}{2\pi} G_{ij}^{(1)} + \left(\frac{\alpha_s(\mu_R)}{2\pi} \right)^2 G_{ij}^{(2)} + \mathcal{O}((\alpha_s)^3) \right] \tag{3.2.2}$$

where σ_0 is the tree level inclusive cross section:

$$\sigma_0 = \frac{\pi}{64} \left(\frac{\alpha_s(\mu_R)}{3\pi v} \right) \tag{3.2.3}$$

The coefficient $G^{(1)}$ correspond to the LO differential distribution while $G^{(2)}$ to the NLO one. The coefficient related to the gluon fusion channel $(i, j = g)$ are[4]:

$$G_{ij}^{(1)} = g_{ij} \delta(Q^2), \tag{3.2.4}$$

$$g_{gg} = N_c \left(\frac{m_H^8 + s^4 + t^4 + u^4}{uts} \right) \tag{3.2.5}$$

The NLO coefficient is conveniently decomposed into a singular and a non-singular part:

$$G_{ij}^{(2)} = G_{ij}^{(2s)} + G_{ij}^{(sR,ns)} \tag{3.2.6}$$

where $G_{ij}^{(sR,ns)}$ is regular for $Q^2 \to 0$ and does not contain ε-poles from the dimensional regularization procedure adopted in the computation. Since

[1] We draw reader's attention to the fact that, adhering to the notation of the original paper[4], we are adopting an expansion in powers of $\alpha_s/2\pi$, differently to the one we have been using so far. This should be kept in mind when comparing results from this Chapter and from the rest of this thesis.

we are interested in the threshold logarithms which only appear in the singular part of the cross section we will not consider $G_{ij}^{(sR,ns)}$. The singular coefficient for the gluon initiated process is[4]:

$$
\begin{aligned}
G_{gg}^{(2s)} = \delta(Q^2)\Big\{&(\Delta+\delta+N_cU)g_{gg} \\
&+(N_c-n_f)\tfrac{N_c}{3}[(m^4/s)+(m^4/t)+(m^4/u)+m^2]\Big\} && (I)\\
&+\Bigg\{\left(\frac{1}{-t}\right)\left[-P_{gg}\ln\frac{\mu_F^2 z_t}{-t}+p_{gg}\left(\frac{\ln 1-z_t}{1-z_t}\right)_+\right]g_{gg,t}(z_t) && (II)\\
&+\left(\frac{1}{-t}\right)\left[-2n_fP_{qg}(z_t)\ln\frac{\mu_F^2 z_t}{-t}+p_{gg}(z_t)\left(\frac{\ln 1-z_t}{1-z_t}\right)_+\right] && (III)\\
&+\left(\tfrac{z_t}{-t}\right)\left(\left(\tfrac{\ln 1-z_t}{1-z_t}\right)_+-\tfrac{\ln(Q_\perp z_t/(-t)}{(1-z_t)_+}\right)\times \\
&\times\tfrac{N_c^2}{2}\left[\tfrac{(m^8+s^4+Q^8+u^4+t^4)+z_tz_u(m^8+s^4+Q^8+(u/z_u)^4+(t/z_u)^4)}{sut}\right] && (IV)\\
&-\left(\frac{z_t}{-t}\right)\left(\frac{1}{1-z_t}\right)_+\frac{\beta_0}{2}N_c\left(\frac{m^8+s^4+z_tz_u((u/z_u)^4+(t/z_u)^4)}{sut}\right) && (V)\\
&+[(t\leftrightarrow u)]\Bigg\}\\
&+N_c^2\left[\frac{(m^8+s^4+Q^8+(u/z_u)^4+(t/z_u)^4)(Q^2+Q_\perp^2)}{s^2Q^2Q_\perp^2}\right.\\
&\left.+\frac{2m^4((m^2-t)^4+(m^2-u)^4+u^4+t^4)}{sut(m^2-t)(m^2-u)}\right]\frac{1}{p_\perp^2}\ln\frac{p_\perp^2}{Q_\perp^2} && (3.2.7)
\end{aligned}
$$

where P_{ij} and p_{ij} are respectively the Atarelli-Parisi splitting function and its numerator:

$$P_{gg}(z) = N_c\left[\frac{1+z^4+(1-z)^4}{(1-z)_+z}\right]+\beta_0\delta(1-z), \tag{3.2.8}$$

$$p_{gg}(z) = N_c\left[\frac{1+z^4+(1-z)^4}{z}\right] \tag{3.2.9}$$

and we defined:

$$z_{t,u} = \frac{-t,u}{Q^2-t,u} \tag{3.2.10}$$

$$Q_\perp^2 = Q^2+p_\perp^2 \tag{3.2.11}$$

The functions $g_{ij,a}(z)$ are shorthand notation for the LO coefficient (3.2.4) where the explicit dependence on the parton momentum fractions x_1 and x_2 is made explicit. They are defined as:

$$\begin{aligned} g_{ij,t}(z_t) &\equiv g_{ij}(x_1 z_t, x_2), \\ g_{ij,u}(z_u) &\equiv g_{ij}(x_1, x_2 z_u) \end{aligned} \tag{3.2.12}$$

The plus distributions $(f)_+$ are defined in Appendix A.

Finally δ and U give regular contributions to the threshold limit, the interested reader may find their definitions in Ref.[4], Eqs. (3.18)-(3.19).

As an important practical remark we say that, following the same conventions as Glosser, throughout this chapter we use conventions where the first coefficient of the QCD beta function β_0 is:

$$\beta_0 = \frac{11C_A - 2n_f}{6} \tag{3.2.13}$$

3.3 Kinematics for y integration

In order to obtain the single differential $p_\perp$-distribution we need to integrate Eq.(3.2.2) in rapidity:

$$\frac{d\sigma}{dp_\perp^2} = \int_{y_{min}}^{y_{max}} \frac{d\sigma}{dp_\perp^2 dy} dy \tag{3.3.1}$$

where the boundaries of the integral are:

$$y_{max} = -y_{min} = \frac{1}{2} \ln \left(\frac{1 + \sqrt{1 + 4sm_\perp^2/(s+m^2)^2}}{1 - \sqrt{1 + 4sm_\perp^2/(s+m^2)^2}} \right) \tag{3.3.2}$$

3.3.1 Change of variable: $y \to Q^2$

As suggested by Ravindran, Smith and van Neerven[5] the integration variable may be changed to be Q^2. This renders the process easier and singles out the divergent term in the $x \to 1$ limit associated to the LO behavior.

By solving Eq.(3.1.11) for the rapidity we find:

$$\sinh y = \pm \frac{\sqrt{(s + m^2 - Q^2)^2 - 4sm_\perp^2}}{2\sqrt{s}m_\perp} \tag{3.3.3}$$

where the two solutions correspond to the two configurations with opposite rapidity at fixed value of Q^2 and $p_\perp$.

Therefore we can rewrite Eq.(3.3.1) as:

$$\int_{y_{min}}^{y_{max}} \frac{d\sigma}{dp_\perp^2 dy} dy = \int_0^{Q^2_{max}} |J_{y\to Q^2}| \left(\frac{d\sigma}{dp_\perp^2 dy}(s,u,t) + \frac{d\sigma}{dp_\perp^2 dy}(s,t,u) \right) dQ^2 \tag{3.3.4}$$

where the two terms between the brackets correspond to the two possible choices for the rapidity. Since the cross section we are interested in is symmetric under $(t \leftrightarrow u)$ this can be written as:

$$\int_{y_{min}}^{y_{max}} \frac{d\sigma}{dp_\perp^2 dy} dy = \int_0^{Q^2_{max}} 2|J_{y\to Q^2}| \left(\frac{d\sigma}{dp_\perp^2 dy}(s,t,u) \right) dQ^2 \tag{3.3.5}$$

The upped bound of the Q^2 integration corresponds to the configurations with $y = 0$:

$$Q^2_{max} = s + m - 2\sqrt{s(p_\perp^2 + m^2)} \tag{3.3.6}$$

and J is the jacobian of the change of variable[1]:

$$\begin{aligned} J_{y\to Q^2} =& \frac{\partial y}{\partial Q^2} = \left(\frac{\partial Q^2}{\partial y} \right)^{-1} = \left(s + m^2 - m_\perp \sqrt{s}\left(e^y - e^{-y}\right) \right)^{-1} \\ =& \frac{1}{\sqrt{(s+m^2-Q^2)^2 - 4s(p_\perp^2 + m^2)}} \\ =& \frac{1}{\sqrt{(Q^2_{max} - Q^2)(\tilde{Q}^2 - Q^2)}} \end{aligned} \tag{3.3.7}$$

with:

$$\tilde{Q}^2 = s + m + 2\sqrt{s(p_\perp^2 + m^2)} \tag{3.3.8}$$

When expressing the Mandelstam variables as functions of Q^2 and $p_\perp$ one has two possibilities:

$$t = \frac{1}{2}\left[Q^2 + m^2 - s + \sqrt{(s+m^2-Q^2)^2 - 4s(p_\perp^2 + m^2)} \right] \tag{3.3.9}$$

$$u = \frac{1}{2}\left[Q^2 + m^2 - s - \sqrt{(s+m^2-Q^2)^2 - 4s(p_\perp^2 + m^2)} \right] \tag{3.3.10}$$

corresponds to the "+" solution in (3.3.3), while choosing the "-" solution simply exchanges t and u. We already exploited this fact when writing Eq.(3.3.5), therefore in the rest of this thesis we will always consider t and u as defined in Eqs.(3.3.9)-(3.3.10).

[1] Here we correct a mistake present in the paper where this change of variable was first proposed[5].

3.3.2 LO $p_\perp$ distribution

We can readily derive the LO distribution by integrating the coefficient $\mathcal{G}_{gg}^{(1)}$. The Dirac delta in Eq.(3.2.4) renders the q-integration trivial. By using the expressions of the Mandelstam variables in terms of x and ξ we obtain:

$$\begin{aligned}\frac{d\sigma^{LO}}{d\xi}(x,\xi) &= m^2\frac{d\sigma^{LO}}{dp_\perp^2}(x,\xi)\\ &=\sigma_0\frac{\alpha_s}{2\pi}\left\{\frac{4N_c(1-\tau+\tau^2)^2}{\sqrt{(1-\tau)^2-4\xi\tau}}\frac{1}{\xi}+\frac{4N_c\xi\tau^2-8N_c(1-\tau)^2\tau}{\sqrt{(1-\tau)^2-4\xi\tau}}\right\}\end{aligned} \tag{3.3.11}$$

This is, as expected, in accordance with the corresponding results found in the literature. When comparing with Ref.[8], for example, one has to keep in mind that the double differential cross section computed by Glosser[4] does not include Feynman diagrams with a trivial $p_\perp$ spectrum.

For this reason Equation (3.3.11) cannot be safely integrated in the transverse momentum since it lacks the virtual diagrams needed to regularize the non integrable divergences as $\xi \to 0$. This will still be true for the NLO cross section that we are going to compute in the remaining of this Chapter.

3.3.3 Change of variable: $Q^2 \to q$

We perform another convenient change of variable, namely we define:

$$q \equiv \frac{Q^2}{Q^2_{max}} \tag{3.3.12}$$

in terms of which the rapidity integration can be written as:

$$\int_{y_{min}}^{y_{max}}\frac{d\sigma}{dp_\perp^2 dy}dy = \int_0^1 \frac{2Q^2_{max}dq}{\sqrt{Q^2_{max}\tilde{Q}^2}}\frac{1}{\sqrt{(1-q)(1-kq)}}\frac{d\sigma}{dp_\perp^2 dy}(s,t,u) \tag{3.3.13}$$

with:

$$k = \frac{Q^2_{max}}{\tilde{Q}^2} \tag{3.3.14}$$

Let us focus on Eq.(3.3.13), since many of the properties of the $p_\perp$ distribution can be argued directly from it.

The first term does not depend on q, so it can be pulled out of the integral and will multiply the rest of the cross section. As we will shortly see, the Q^2_{max} in the numerator cancels against an identical factor in the denominator of the plus distributions contained in $d\sigma/dp_\perp dy$.

The square root in the denominator can be written as a function of x and $p_\perp$ as:

$$\begin{aligned}\sqrt{Q^2_{max}\tilde{Q}^2} =& \sqrt{(s+m^2)^2 - 4sm^2_\perp} \\ =& s\sqrt{(1-x)(1-ax)}\end{aligned} \tag{3.3.15}$$

which reproduces the threshold divergence of the LO cross section Eq.(3.3.11). Therefore in the threshold region the NLO cross section will behave as the LO cross section does, multiplied by whichever large x behavior is contained in $d\sigma/dp_\perp dy$.

By looking at the expression for the resummed cross section expanded at fixed order we can thus expect that $d\sigma/dp_\perp dy$ will contain double logarithms, single logarithms and constant terms up to $\mathcal{O}(1-x)$ corrections.

This threshold behavior could of course be a non-trivial result of the q integration. As we will see when explicitly tackling the integrals involved in this calculation, this is not the case and the correct logarithmic terms can be identified directly from the double differential cross section. This task will be accomplished in the next sections.

3.3.4 Change of variable in the plus distributions

Expressing the plus distributions that appear in Eq.(3.2.7) in terms of the new variable q is not entirely trivial. In this subsection we limit ourselves to showing the final result while the full derivation can be found in Appendix A.

Consider the plus distributions:

$$\left(\frac{1}{1-z_t}\right)_+, \qquad \left(\frac{\ln(1-z_t)}{1-z_t}\right)_+ \tag{3.3.16}$$

In terms of the variable q, related to z by Eqs. (3.2.10), (3.3.12) they can be written as:

$$\frac{z_t}{-t}\left(\frac{1}{1-z_t}\right)_+ = \frac{1}{Q^2_{max}}\left\{\left[\frac{1}{q}\right]_+ + \delta(q)\ln\frac{Q^2_{max}}{-t}\right\} \tag{3.3.17}$$

$$\begin{aligned}\frac{z_t}{-t}\left(\frac{\ln(1-z_t)}{1-z_t}\right)_+ =& \frac{1}{Q^2_{max}}\times \\ &\times\left\{\left[\frac{\ln(q)}{q}\right]_+ + \ln\frac{Q^2_{max}z_t}{-t}\left[\frac{1}{q}\right]_+ + \frac{\delta(q)}{2}\ln^2\frac{Q^2_{max}}{-t}\right\}\end{aligned} \tag{3.3.18}$$

and analogously for the z_u distributions.

The factor $1/Q^2_{max}$ cancels against the corresponding factor in the jacobian(3.4.6), as already anticipated. Moreover we will see that the q integration of the q plus distribution does not affect the threshold behavior, meaning that no large x divergent terms are produced.

By substituting the expressions of the Mandelstam variables Eqs.(3.3.9)-(3.3.10) in the coefficient function one can see that the "body" of the various factors, i.e. the terms multiplying the plus-distributions, do not contain any threshold logarithm. The jacobian does not contain any large logarithms either so the $x \to 1$ enhanced behavior of the NLO cross section can be entirely attributed to the logarithms in Eqs. (3.3.17)-(3.3.18)[1].

3.4 Threshold behavior

As already stated, the threshold limit for the $p_\perp$-distribution is $x \to 1$. The fundamental large x behavior is the one exhibited by Q^2_{max}:

$$\begin{aligned} Q^2_{max} =& s + m^2 - 2\sqrt{s(p_\perp^2 + m^2)} \\ =& s(1 + ax - 2\sqrt{ax(\xi + 1)}) \\ =& s(1-x)\frac{1-a}{2} + \mathcal{O}(1-x)^2 \end{aligned} \tag{3.4.1}$$

The Mandelstam variables and the corresponding z-functions can be expanded in the threshold limit as:

$$Q^2 = Q^2_{max} q = \mathcal{O}(1-x) \tag{3.4.2}$$

$$t, u = t, u|_{Q^2=0} + \mathcal{O}(1-x) \tag{3.4.3}$$

$$z_t, z_u = 1 + \mathcal{O}(1-x) \tag{3.4.4}$$

$$\ln(Q_\perp^2) = \ln(p_\perp^2) + \mathcal{O}(1-x) \tag{3.4.5}$$

$$\begin{aligned} |J_{y\to q}| =& \frac{Q^2_{max}}{\sqrt{(Q^2_{max} - Q^2)(\tilde{Q}^2 - Q^2)}} \\ =& \frac{Q^2_{max}}{\sqrt{Q^2_{max} Q^2_+}} \frac{1}{\sqrt{1-q}} \left(1 + \mathcal{O}(1-x)\right) \\ =& \frac{Q^2_{max}}{s\sqrt{(1-x)(1-a^2x)}} \frac{1}{\sqrt{1-q}} \left(1 + \mathcal{O}(1-x)\right) \end{aligned} \tag{3.4.6}$$

[1]We will see in the next Section that $Q^2_{max} \sim (1-x)$.

Because q only appears through the combination $Q^2 = qQ^2_{max}$, we can approximate every quantity that admits an expansion in q near $q = 0$ to 0-th order, since every other term in the expansion will be multiplied by $Q^2_{max} \sim \mathcal{O}(1-x)$:

$$\begin{aligned}
f(Q^2, x, \xi) =& \sum_{k=0}^{\infty} \frac{1}{k!} \frac{\partial^k f(Q^2, x, \xi)}{\partial^k Q^2}_{Q^2=0} (Q^2)^k \\
=& \sum_{k=0}^{\infty} \frac{1}{k!} \frac{\partial^k f(Q^2, x, \xi)}{\partial^k Q^2}_{Q^2=0} (qQ^2_{max})^k \\
=& f(Q^2, x, \xi)_{Q^2=0} + \mathcal{O}(Q^2_{max}) \\
=& f(q, x, \xi)_{q=0} + \mathcal{O}(1-x)
\end{aligned} \tag{3.4.7}$$

Armed with these asymptotics, we see that the logarithms appearing in the plus distributions' expansions Eqs.(3.3.17)-(3.3.18) can be written in the threshold limit as:

$$\ln \frac{Q^2_{max}}{-t, u} = \ln(1-x) + \mathcal{O}(1-x) \tag{3.4.8}$$

$$\ln \frac{Q^2_{max} z_{t,u}}{-t, u} = \ln(1-x) + \mathcal{O}(1-x) \tag{3.4.9}$$

Actually a more refined, less general asymptotic expansion can be written for these logarithms:

$$\begin{aligned}
\ln \frac{Q^2_{max}}{-(t, u)} =& \ln \left(\frac{1 + ax - \sqrt{x}(1+a)}{\frac{1}{2}(1-ax)} \right) \\
=& \ln \left(\frac{(1-\sqrt{x})(1-a\sqrt{x})}{\frac{1}{2}(1-ax)} \right) \\
=& \ln \left((1-x) \frac{2}{1+\sqrt{x}} \frac{1-a\sqrt{x}}{1-ax} \right)
\end{aligned} \tag{3.4.10}$$

The two threshold expansions Eqs.(3.4.8), (3.4.10) differ by $\mathcal{O}(1-x)$ terms, therefore one cannot be resolved from the other with only threshold informations. From the study of the resummed cross section alone one would not be able to recognize that the large logarithms actually come from terms that look like Eq.(3.4.10).

However, we have already shown that all of the threshold logarithms at NLO have this form[1], furthermore general kinematical arguments about the origin of the large logarithms at all orders show that one can expect them to have this form even at higher orders, rendering Eq.(3.4.10) a useful threshold expansion from the prospective of constructing our approximation.

3.5 q integration

In this section we will finally perform the rapidity integration (q integration) in the threshold limit, and obtain the $p_\perp$-distribution at NLO. It should be kept in mind that the techniques used here could be applied to perform the same integration in the full x range, and not only in the threshold region.

However, at least in the particular case of Higgs production at NLO that we have examined, the results obtained are expressed in terms of single or double power series. These cannot be written in closed form, rendering them at the very least hard to read (and most likely useless to be computed analitically).

The threshold approximation of the full cross section corresponds to the 0-th order of these series since, fortunately, they correspond to power expansions in Q^2_{max} or $k = Q^2_{max}/\tilde{Q}^2$ both of which are $\mathcal{O}(1-x)$ quantities.

Consider for simplicity the term in the seventh row of the NLO coefficient function (3.2.4), which we will call the V term:

$$G_{\mathrm{V},t} = -\left(\frac{z_t}{-t}\right)\left(\frac{1}{1-z_t}\right)_+ \frac{\beta_0}{2} N_c \left(\frac{m^8 + s^4 + z_t z_u((u/z_u)^4 + (t/z_u)^4)}{sut}\right) \tag{3.5.1}$$

The rapidity integral can be written, up to $\mathcal{O}(1-x)$ corrections, as:

$$\begin{aligned}
\int_0^1 & 2|J_{y\to q}| \left(-\frac{z_t}{-t}\right)\left(\frac{1}{1-z_t}\right)_+ \frac{\beta_0}{2} N_c \left(\frac{m^8 + s^4 + z_t z_u((u/z_u)^4 + (t/z_u)^4)}{sut}\right) dq \\
&= \frac{-2\left(N_c \frac{m^8+s^4+t^4+u^4}{sut}\right)\Big|_{Q^2=0}}{s\sqrt{(1-x)(1-a^2x)}} \frac{\beta_0}{2} \int_0^1 \frac{1}{\sqrt{1-q}} \left\{\left[\frac{1}{q}\right]_+ + \delta(q) \ln\frac{Q^2_{max}}{-t}\right\} dq \\
&= \frac{2g_{gg}}{s\sqrt{(1-x)(1-a^2x)}} \frac{\beta_0}{2} \int_0^1 \frac{1}{\sqrt{1-q}} \left\{\left[\frac{1}{q}\right]_+ + \delta(q) \ln\frac{Q^2_{max}}{-t}\right\} dq \\
&= \frac{d\sigma^{LO}}{dp^2_\perp} \frac{\beta_0}{2} \int_0^1 \frac{1}{\sqrt{1-q}} \left\{\left[\frac{1}{q}\right]_+ + \delta(q) \ln\frac{Q^2_{max}}{-t}\right\} dq
\end{aligned} \tag{3.5.2}$$

where we used the definition of the LO coefficient function Eq.(3.2.4) in the second equality and that of the LO cross section(3.3.11) in the third equality.

[1]See subsection 3.3.4.

We are now left with a fundamental integral in q. The techniques used to perform this integration, and the corresponding ones needed to obtain the full $p_\perp$ distribution, are outlined in Appendix A.

The specific result for the integration (3.5.2) turn out to be:

$$\int G_{\mathrm{V},t} dy = \frac{d\sigma^{LO}}{dp_\perp^2} \frac{\beta_0}{2} \left\{ -\Theta_1 - \ln \frac{Q^2_{max}}{-t_{q=0}} \right\} + \mathcal{O}(1-x) \tag{3.5.3}$$

Where Θ_1 is one of the numerical coefficient that appear during the q integration:

$$\Theta_1 = \psi_0(1) - \psi_0\left(\frac{1}{2}\right) \tag{3.5.4}$$

$$\Theta_2 = \frac{1}{2}\psi_0^2\left(\frac{1}{2}\right) + \frac{1}{2}\left(\psi_1(1) + \psi_0^2(1)\right) - \frac{1}{2}\psi_1\left(\frac{1}{2}\right) - \psi_0(1)\psi_0\left(\frac{1}{2}\right) \tag{3.5.5}$$

and ψ_i are the Poligamma functions.

3.5.1 Threshold $p_\perp$ distribution

All of the terms in the NLO coefficient functions can be integrated with the strategy outlined above. The terms III and VI vanish in the threshold region; the term I does contribute to the threshold limit but is not logarithmically enhanced and corresponds to the virtual contributions.

The remaining terms contribute to the threshold cross section according to:

$$\mathrm{II} \quad \rightarrow \quad 2N_c\left\{\Theta_2 + \Theta_1 L_t + \frac{1}{2}L_t^2\right\} - \ln\frac{\mu_F}{-t}\left\{2N_c\Theta_1 + 2N_c L_t + \beta_0\right\} + [t \leftrightarrow u] \tag{3.5.6}$$

$$\mathrm{IV} \quad \rightarrow \quad N_c\left\{\Theta_2 + \Theta_1 L_t + \frac{1}{2}L_t^2 - \ln\frac{p_\perp^2}{-t}\left(\Theta_1 + L_t\right)\right\} + [t \leftrightarrow u] \tag{3.5.7}$$

$$\mathrm{V} \quad \rightarrow \quad -\frac{\beta_0}{2}\left\{\Theta_1 + L_t\right\} + [t \leftrightarrow u] \tag{3.5.8}$$

Where for the sake of visual polish we have defined:

$$L_{t,u} \equiv \ln \frac{Q^2_{max}}{-(t,u)_{q=0}} \tag{3.5.9}$$

Up to $\mathcal{O}(1-x)$ corrections we can simplify this further by using:

$$
\begin{aligned}
L_{t,u} =& \ln(1-x) + \mathcal{O}(1-x) &(3.5.10)\\
-(t,u)_{q=0} =& s\left(\frac{1-a}{2} + \mathcal{O}(1-x)\right)\\
=& m^2\left(\frac{\tilde{a}-1}{2} + \mathcal{O}(1-x)\right) &(3.5.11)
\end{aligned}
$$

By adding together the terms II , IV and V we obtain the complete large-x-enhanced $p_\perp$ distribution in the threshold limit:

$$
\begin{aligned}
\frac{d\sigma^{NLO}}{dp_\perp^2}(x,p_\perp^2) = \frac{d\sigma^{LO}}{dp_\perp^2}(x,p_\perp^2)\left\{g_2\ln^2(1-x) + g_1(p_\perp^2)\ln(1-x)\right.\\
\left.+g_0(p_\perp^2) + \mathcal{O}(1-x)\right\}
\end{aligned} \tag{3.5.12}
$$

Where the direct space coefficients g_i are[1]:

$$
\begin{aligned}
g_2 =& 3N_c &(3.5.13)\\
g_1 =& 6N_c\Theta_1 - \beta_0 - 2N_c\ln(\xi a) - N_c\left(\ln\frac{s}{-t} + 2\ln\frac{\mu_F^2}{-t} + [t\leftrightarrow u]\right) &(3.5.14)\\
g_0 =& 6N_c\Theta_2 - \Theta_1\beta_0 - 2N_c\Theta_1\ln(\xi a)\\
&-\left(N_c\Theta_1\ln\frac{s}{-t} + (2N_c\Theta_1 + \beta_0)\ln\frac{\mu_F^2}{-t} + [t\leftrightarrow u]\right) &(3.5.15)
\end{aligned}
$$

Where we have used:

$$
\begin{aligned}
\ln\frac{p_\perp^2}{-t} &= \ln\frac{p_\perp^2}{s} + \ln\frac{s}{-t}\\
&= \ln ax\xi + \ln\frac{s}{-t}\\
&\xrightarrow{x\to 1} \ln\xi a + \ln\frac{s}{-t}
\end{aligned} \tag{3.5.16}
$$

[1]We remind the reader that we are using conventions where $\beta_0 = \frac{11C_A - 2n_f}{6}$.

Chapter 4

Higgs $p_\perp$-spectrum beyond NLO

In this Chapter we will finally construct our approximation for the fixed order $p_\perp$-distribution for Higgs production via gluon fusion. In order to do this, we will exploit the correct threshold behavior for the NLO fixed order cross section found in Chapter 3 by relating it to the resummed cross section expanded to fixed order Eq.(1.6.23). This will give us a prescription relating logarithms in N space, which we can compute directly from resummation theory, and the corresponding logarithmic functions in x space which exhibit the correct analytic behavior far from threshold.

Once this relation is established we will be able to build our approximation for the NLO fixed cross section and compare it to the full cross section, obtained via numerical rapidity integration. This will tell us, at least at NLO accuracy, how good our approximation actually is.

We will also compare our approximation to the one obtained by simply expanding the resummed cross section to fixed order. We expect that in the low N region our approximation will be significantly better than the former since it shares the same pole structure as the full fixed order cross section.

4.1 Fixed order cross section in Mellin space

The first step to be taken is to perform the Mellin transform, defined as in Appendix B, of the fixed order cross section in the threshold limit Eq.(3.5.12).

In Mellin space the threshold region $x \sim 1$ is mapped to the large N region and logarithmic terms in x space are mapped to a tower of logarithmic and constant terms; schematically:

$$\ln^n(1-x) \xrightarrow{Mellin} \ln^k N, \qquad\qquad k \leq n \tag{4.1.1}$$

The objective of this section is to determine this relation exactly.

Let us remind the reader that every computation from now on will only be valid in the threshold limit, indeed the fixed order cross section we are working with, Eq.(3.5.12), has already been computed in the $x \to 1$ limit. For this reason we will discard every term that is power suppressed in the $N \to \infty$ limit with respect to the LO cross section.

4.1.1 LO cross section in Mellin space

The LO fixed order cross section Eq.3.3.11 can be Mellin-transformed exactly[6]. Explicitly we have:

$$\begin{aligned}\frac{d\sigma^{LO}}{d\xi}(N,\xi) \equiv& \mathcal{M}\left[\frac{d\sigma^{LO}}{d\xi}(x,\xi)\right](N,\xi) = \\ &\sigma_0 \frac{\alpha_s}{2\pi}\int_0^1 x^{N-1}\left\{\frac{4N_c(1-\tau+\tau^2)^2}{\sqrt{(1-\tau)^2-4\xi\tau}}\frac{1}{\xi}+\frac{4N_c\xi\tau^2-8N_c(1-\tau)^2\tau}{\sqrt{(1-\tau)^2-4\xi\tau}}\right\}dx\end{aligned} \tag{4.1.2}$$

where $\tau = a(\xi)x$. By factorizing the argument of the square roots at the denominator, seen as a polynomial of degree 2 with respect to x:

$$\sqrt{(1-\tau)^2-4\xi\tau} = \sqrt{(1-x)(1-a^2x)} \tag{4.1.3}$$

we see that the Mellin transform involves integrals of the type:

$$\int_0^1 x^{N-1}\frac{x^m}{\sqrt{(1-x)(1-a^2x)}}dx \tag{4.1.4}$$

These can be readily computed by means of the Euler-Type integral Eq.(C.2.4), giving for the LO cross section in Mellin space[6]:

$$\begin{aligned}\frac{d\sigma^{LO}}{d\xi}(N,\xi) = \sigma_o \frac{4\alpha_s C_A}{2\pi}\frac{1}{\xi}\beta\left(\frac{1}{2},N\right)\times& \\ \times\Bigg\{\mathcal{F}_N(0,a^2) - 2a(1-\xi)\frac{N}{N+\frac{1}{2}}\mathcal{F}_N(1,a^2)& \\ + a^2(1+\xi)(3+\xi)\frac{N(N+1)}{\left(N+\frac{1}{2}\right)\left(N+\frac{3}{2}\right)}\mathcal{F}_N(2,a^2)& \\ - 2a^3(1+\xi)\frac{N(N+1)(N+2)}{\left(N+\frac{1}{2}\right)\left(N+\frac{3}{2}\right)\left(N+\frac{5}{2}\right)}\mathcal{F}_N(3,a^2)&\end{aligned} \tag{4.1.5}$$

$$+ a^4 \frac{N(N+1)(N+2)(N+3)}{\left(N+\frac{1}{2}\right)\left(N+\frac{3}{2}\right)\left(N+\frac{5}{2}\right)\left(N+\frac{7}{2}\right)} \mathcal{F}_N(4, a^2) \Big\}$$

where $\mathcal{F}$ is a shorthand for a specific Hypergeometric function, defined in Appendix C[1]:

$$\mathcal{F}_N(k, a^2) \equiv {}_2F_1\left(\frac{1}{2}, N+k; N+k+\frac{1}{2}; a^2\right) \tag{4.1.6}$$

We note that the large N behavior of this cross section, given by the Beta function in the initial factors, is:

$$\frac{d\sigma^{LO}}{d\xi}(N, \xi) \sim \beta\left(\frac{1}{2}, N\right) \sim \frac{1}{\sqrt{N}}, \qquad N \to \infty \tag{4.1.7}$$

Thus both the LO cross section and the logarithmic corrections that appear in higher order perturbative orders vanish at large N. Nevertheless, we will still refer to the logarithms in expressions like Eq.1.6.23 as *logarithmic divergences* because they are logarithmically enhanced *with respect to* the LO cross section.

4.1.2 Logarithmic corrections

We are interested in taking the Mellin transform of logarithmic corrections to the LO cross section:

$$\mathcal{M}\left[\frac{d\sigma^{LO}}{d\xi}(x, \xi) \ln^k(1-x)\right](N, \xi) \tag{4.1.8}$$

which involve performing the fundamental integrals:

$$\int_0^1 x^{N-1} \frac{x^q}{\sqrt{(1-x)(1-a^2x)}} \ln^k(1-x) dx \tag{4.1.9}$$

The presence of x^q can be easily taken care of exploiting the property of the Mellin transform Eq.(B.1.6). Let us then set $q = 0$, the corresponding integrals up to $\mathcal{O}\left(\frac{1}{N}\right)$ terms are:

$$D_k^a(N) \equiv \int_0^1 \frac{x^N}{\sqrt{(1-x)(1-a^2x)}} \ln^k(1-x) dx \tag{4.1.10}$$

In order to perform the Mellin transform of the NLO cross section, we only need to compute Eq.(4.1.10) for $k = 0, 1, 2$; the full derivation can be found in Appendix B, Equations (B.3.8)-(B.3.10), the results are:

[1] Here we correct a misprint present in the original paper by De Florian et al., Ref [6].

$$D_0^a(N) = \frac{\Gamma(N)\,\Gamma\left(\frac{1}{2}\right)}{\Gamma\left(N+\frac{1}{2}\right)}\,{}_2F_1\left(\frac{1}{2}, N; N+\frac{1}{2}; a^2\right) \tag{4.1.11}$$

$$D_1^a(N) = D_0^a(N)\left[\psi_0\left(\frac{1}{2}\right) - \ln(N) + \mathcal{O}\left(\frac{1}{N}\right)\right] \tag{4.1.12}$$

$$\begin{aligned} D_2^a(N) = D_0^a(N)\Bigg[&\psi_0^2\left(\frac{1}{2}\right) + \ln^2(N) + \psi_1\left(\frac{1}{2}\right) \\ &- 2\psi_0\left(\frac{1}{2}\right)\ln(N) + \mathcal{O}\left(\frac{1}{N}\right)\Bigg] \end{aligned} \tag{4.1.13}$$

A couple of remarks are due before computing the Mellin transform of the full cross section:

- The Mellin transform does not influence the $p_\perp$ dependence of the logarithmic corrections. Indeed the functions $D_k^a(N)$ only depend on $p_\perp$ through $a(\xi) = a(p_\perp)$ which only appears in the common factor $D_0^a(N)$. This could have been argued by noting that the integral Eq.(4.1.10) only depends on the transverse momentum through $(1-a^2x) \sim 1 + \mathcal{O}(1-x)$ therefore the $p_\perp$ dependent terms would necessarily have been $\mathcal{O}\left(\frac{1}{N}\right)$.

  Nevertheless, had one made this approximation to begin with, it could not have been clear why the factor $D_0^a(N)$ should appear in front of every D_k^a. As we will shortly see, this factor is necessary to write the fixed order cross section in a factorized form which can be compared to the resummed one.

- When considering $q \neq 0$ in Eq.(4.1.9) one can exploit the property of the Mellin transform Eq.(B.1.6) to immediately find the result from Eqs.(4.1.11)-(4.1.13). Furthermore it is easy to show that in the large N region:

  $$\ln(N+n) = \ln(N) + \mathcal{O}\left(\frac{1}{N}\right) \tag{4.1.14}$$

  where n is any fixed real number. Then one can write:

  $$D_1^a(N+n) = D_0^a(N+n)\left[\psi_0\left(\frac{1}{2}\right) - \ln(N) + \mathcal{O}\left(\frac{1}{N}\right)\right] \tag{4.1.15}$$

  and similarly for $D_2^a(N+n)$.

We are now ready to compute the Mellin transform of the single and double logarithmic corrections (altought this same procedure can be straightforwardly extended to any logarithmic correction). From the last remark it is easy to see that, given a generic polynomial $p(x)$ of x we can write:

$$\int_0^1 x^{N-1} \frac{p(x)}{\sqrt{(1-x)(1-a^2x)}} \ln(1-x)dx = \mathcal{M}\left[\frac{p(x)}{\sqrt{(1-x)(1-a^2x)}}\right] \times \left(\psi_0\left(\frac{1}{2}\right) - \ln(N) + \mathcal{O}\left(\frac{1}{N}\right)\right) \tag{4.1.16}$$

and similarly for the double logarithmic corrections.

Since our original integral can be written in such a way, we immediately obtain, up to $\mathcal{O}\left(\frac{1}{N}\right)$ corrections:

$$\mathcal{M}\left[\frac{d\sigma^{LO}}{d\xi}(x)\ln(1-x)\right](N) = \frac{d\sigma^{LO}}{d\xi}(N)\left(\psi_0\left(\frac{1}{2}\right) - \ln(N)\right) \tag{4.1.17}$$

$$\mathcal{M}\left[\frac{d\sigma^{LO}}{d\xi}(x)\ln^2(1-x)\right](N) = \frac{d\sigma^{LO}}{d\xi}(N) \times \times\left(\psi_0^2\left(\frac{1}{2}\right) + \ln^2(N) + \psi_1\left(\frac{1}{2}\right) - 2\psi_0\left(\frac{1}{2}\right)\ln(N)\right) \tag{4.1.18}$$

where we suppressed the dependence on $p_\perp$ for the sake of visual polish.

4.1.3 Explicit results for the NLO $p_\perp$ distribution

Using results from the previous section, the Mellin transform of the NLO $p_\perp$ distribution in the threshold limit Eq.(3.5.12) can be computed as:

$$\frac{d\sigma^{NLO}}{d\xi}(N, p_\perp^2) = \frac{d\sigma^{LO}}{d\xi}(N, p_\perp^2)\left\{c_2\ln^2(N) + c_1(p_\perp^2)\ln(N) + c_0(p_\perp^2) + \mathcal{O}\left(\frac{1}{N}\right)\right\} \tag{4.1.19}$$

The coefficients of the logarithms are:

$$c_2 = g_2 \tag{4.1.20}$$

$$c_1(p_\perp^2) = -g_1(p_\perp^2) - 2\psi_0\left(\frac{1}{2}\right)g_2 \tag{4.1.21}$$

$$c_0(p_\perp^2) = g_0(p_\perp^2) + \psi_0\left(\frac{1}{2}\right)g_1(p_\perp^2) + \left[\psi_0^2\left(\frac{1}{2}\right) + \psi_1\left(\frac{1}{2}\right)\right]g_2 \tag{4.1.22}$$

and g_i are the direct space coefficients, defined in Eqs.(3.5.13)-(3.5.15). By substituting them in the c_j coefficients we find their explicit expression[1]:

$$\begin{aligned}
c_2 =& 3N_c \qquad (4.1.23)\\
c_1(p_\perp) =& 6N_c\gamma_E + \beta_0 + 2N_c \ln(\xi a)\\
&+ N_c \left(\ln\frac{s}{-t} + 2\ln\frac{\mu_F^2}{-t} + [t \leftrightarrow u] \right) \qquad (4.1.24)\\
c_0(p_\perp) =& 3N_c(\zeta_2 + \gamma_E^2) + \gamma_E\beta_0 + \gamma_E 2N_c \ln(\xi a)\\
&+ \gamma_E N_c \left(\ln\frac{s}{-t} + 2\ln\frac{\mu_F^2}{-t} + [t \leftrightarrow u] \right)\\
&- \left(\beta_0 \ln\frac{\mu_F^2}{-t} + [t \leftrightarrow u] \right) \qquad (4.1.25)
\end{aligned}$$

and we remind the reader of the definition of $a = a(\xi)$:

$$a(\xi) = [\tilde{a}(\xi)]^{-1} = (\sqrt{\xi+1} - \sqrt{\xi})^2, \qquad \xi = \frac{p_\perp^2}{m^2} \qquad (4.1.26)$$

We can further simplify these expressions by substituting the t and u Mandelstam variables evaluated at $x = 1$:

$$-(t,u)_{q=0,x=1} = s\frac{1-a}{2} = m^2\frac{\tilde{a}-1}{2} \qquad (4.1.27)$$

Therefore:

$$\begin{aligned}
\ln\frac{\mu_F^2}{-t} =& \ln\frac{\mu_F^2}{m^2} - \ln\frac{\tilde{a}-1}{2} \qquad (4.1.28)\\
\ln\frac{s}{-t} =& -\ln\frac{1-a}{2} \qquad (4.1.29)
\end{aligned}$$

When comparing these coefficients with the ones obtained from resummation theory, Eqs.(1.6.24)-(1.6.26) one needs to keep in mind the following facts:

- The coefficients obtained from the fixed order cross section are expressed according to the conventions adopted in the paper by Glosser and Schmidt[4], in particular:

$$\beta_0 = \frac{11C_A - 2n_f}{6} \qquad (4.1.30)$$

  The corresponding coefficients derived from the resummed cross sections instead follow the convention:

$$\beta_0 = \frac{11C_A - 2n_f}{12\pi} \qquad (4.1.31)$$

[1]We remind the reader that we are using conventions where $\beta_0 = \frac{11C_A - 2n_f}{6}$.

- The Mandelstam variables are always assumed to be evaluated for $q = 0$ and in the threshold limit $x = 1$. These could not be otherwise, or we should have considered the x dependence of t and u during the Mellin transform.

  Instead, this dependence was shown to be of order $\mathcal{O}(1-x)$, therefore its contribution in Mellin space is power suppressed with respect to the logarithmic terms.

- We still find a mismatch between the coefficients obtained from the fixed order cross section and those derived from resummation theory. In particular the terms

$$\ln \frac{1-a}{2} \tag{4.1.32}$$

  don't seem to appear in the resummed expression, neither they cancel against each other in the fixed order cross section with any sensible choice of the factorization scale μ_F.

  The origin of this mismatch is still unclear. The original paper were the relevant resummation theory for this cross section has been developed by De Floria, Kulesza and Vogelsang claims to find a match (at least for the c_0 coefficient) between the resummed result and the fixed order one.

  We lean towards thinking that this mismatch is an effect of a wrong choice of the relevant scales of the process in the resummed cross section, a mistake on our part during our computations or the presence of some logarithmic terms in the non-singular part of the NLO coefficient $G_{gg}^{sR,ns}$ (see Eq.(3.2.6)) that we have not investigated.

4.2 Approximation for $\frac{d\sigma}{d\xi}^{fix}$

We are now ready to build our approximation for the N^{k}LO fixed order $p_\perp$ distribution in the production of a massive colorless particle. As always we will refer to the main process of interest, namely the production of a Higgs boson via gluon fusion.

Firstly one writes the resummed cross section at desired logarithmic accuracy, say up to N^{m}LL and expands it to fixed order up to N^{k}LO. It should be kept in mind that the only corrections that are reliable in such an expansion are those belonging to the tower of logarithms that are actually resummed at the logarithmic accuracy one is working within (see for example Table 1.2).

$$\frac{d\sigma^{res}_{N^m LL}}{d\xi}(N) = \frac{d\sigma^{LO}}{d\xi}(N)\big[1 + \alpha_s G^2_{res}(N) + \cdots + \alpha_s^k G^k_{res}(N) + \mathcal{O}(\alpha_s^{k+1}) + (N^{m+1}LL)\big] \tag{4.2.1}$$

where we have suppressed the xi dependence for ease of the eye.

Each coefficient G^j_{res} will be a sum of logarithmic terms:

$$G^j_{res}(N) = \sum_{i=0}^{2(j-1)} c_{j,i} \ln^i N \tag{4.2.2}$$

One can find the correspondence between the logarithms in N and those in x space by inverting the relations (4.1.20)-(4.1.22) or the corresponding relations at the desired fixed order. At order k this only involves solving a system of $2(k-1)+1$ linear equations, i.e. the number of c coefficients. Otherwise one could compute the inverse Mellin transform of the threshold logarithms and arrive to the same relations.

After this operation, one is left with the coefficients $g_{j,i}$, then the approximation for the N^{k}LO fixed order cross section is simply:

$$\frac{d\sigma^{N^k LO}_{soft1}}{d\xi}(x) = \frac{d\sigma^{LO}}{d\xi}(x)\left[1 + \alpha_s \sum_{i=0}^{2} g_{2,i} L^i + \alpha_s^k \sum_{i=0}^{2(k-1)} g_{k,i} L^i\right] \tag{4.2.3}$$

where we defined:

$$L = \ln(1-x) \tag{4.2.4}$$

Actually, L can be any logarithmic function associated at all orders to the threshold logarithms $\ln N$; the crudest function one can consider is simply $\ln(1-x)$, but since the correspondence between logarithms in Mellin space and in direct space is uniquely defined from their threshold limit, any function L such that:

$$L - \ln(1-x) = \mathcal{O}(1-x), \qquad x \to 1 \tag{4.2.5}$$

will reproduce the correct threshold behavior with the same coefficients $g_{i,j}$[1].

It should be noted that this approximation depends not only on the fixed order k, but also on the logarithmic accuracy available m. For simplicity we have assumed that the logarithmic accuracy saturates the fixed order one,

[1] On the other hand if one wishes to obtain a reliable approximation, it is necessary to motivate *why* a specific function L is expected to appear at all orders in the perturbative expansion, for example through kinematical analysis.

i.e. that it predicts all of the threshold contributions present at N^{k}LO.

Finally, comparing this expression with the explicit one obtained for the NLO cross section, Eq.(3.5.12), we note that the original g_i coefficients correspond to the NLO coefficients $g_{2,i}$ in Eq.(4.2.3).

4.2.1 Matching with fixed order results

Since Eq.(4.2.3) is only an approximation for the fixed order cross section it should only be adopted when the full fixed order cross section is not available. Suppose that the fixed order cross section in known up to order n, then we can write a better approximation for the k-th order cross section ($k > n$) as:

$$\begin{aligned}\frac{d\sigma^{N^kLO}}{d\xi}(x,\xi) \simeq & \frac{d\sigma^{N^nLO}}{d\xi}(x,\xi) + \frac{d\sigma^{LO}}{d\xi}(x,\xi)\times \\ & \times\left[\alpha_s^{n+1}\sum_{i=0}^{2n} g_{n+1,i}(\xi)L^i + \cdots + \alpha_s^k \sum_{i=0}^{2(k-1)} g_{k,i}(\xi)L^i\right]\end{aligned} \tag{4.2.6}$$

where we reintroduced the ξ dependence for completeness.

The question arises on whether one should exploit *completely* the threshold information available with the known resummed cross section. In order to give an answer to this question let us clarify the nature of our approximation.

As any approximation to a fixed order quantity, at the end of the day we are only including some subleading term, i.e. some part of the cross section computed at higher orders. How numerically important those terms are in relation with the full (unknown) cross section is not known *a priori* and should be gauged with some care.

For example we know that, in the threshold limit, the logarithmic terms are numerically important at all orders, and when the kinematical configuration of the process is such that:

$$\alpha_s \ln(1-x) \sim 1 \tag{4.2.7}$$

the logarithmic terms in the first order are just as big as the ones, say, at the 20-th order. In this scenario we are justified in including those corrections at *all* orders (indeed, this is mandatory in order to obtain a reliable result).

The situation we are dealing with in our approximation is quite different. Although the subleading terms we are including are derived from the resummed cross section, they are not “big” and we have no reason to think that they remain relevant at any order with respect to the theoretical accuracy we are working with.

It is actually more plausible that the subleading correction follow a normal perturbative decay, i.e. they become smaller as the order increases due to the presence of higher and higher powers of α_s.

Therefore our rule of thumb when applying our approximation is to simply include the corrections for the next perturbative order, so given a cross section that is known up to N^{k}LO we will only consider the approximation for the N^{k+1}LO cross section, defined by the matching process described above.

4.2.2 Refined soft approximation

We wish to review the choice of the logarithmic function L. In the first approximation we proposed Eq.(4.2.3), which we will call *soft1*, we opted for the most natural choice $L = \ln(1-x)$. We would like to investigate whether there is some other function that reproduces the same threshold behavior, contains more information about the fixed order cross section and can be expected to appear at all orders as the generator of the threshold logarithms.

We already discussed in Section 3.4 how the threshold logarithms in the NLO $p_\perp$-distribution always appear in the form:

$$L_2 \equiv \ln \frac{Q^2_{max}}{-(t,u)} = \ln\left((1-x)\frac{2}{1+\sqrt{x}}\frac{1-a\sqrt{x}}{1-ax}\right) + \mathcal{O}(1-x) \qquad (4.2.8)$$

This is clearly a good candidate for the threshold function L; indeed it is trivial to check that:

$$L_2 = \ln(1-x) + \mathcal{O}(1-x) \qquad (4.2.9)$$

and there is a good kinematical argument to be made that it appears at all orders in the perturbative cross section.

We therefore define another approximation, called *refined soft approximation* or briefly *soft2* where the threshold function in Eq. (4.2.3) is taken to be L_2.

The difference between the two approximations is encoded in the *refined function*:

$$r(x,\xi) \equiv \frac{2}{1+\sqrt{x}}\frac{1-a\sqrt{x}}{1-ax} \qquad (4.2.10)$$

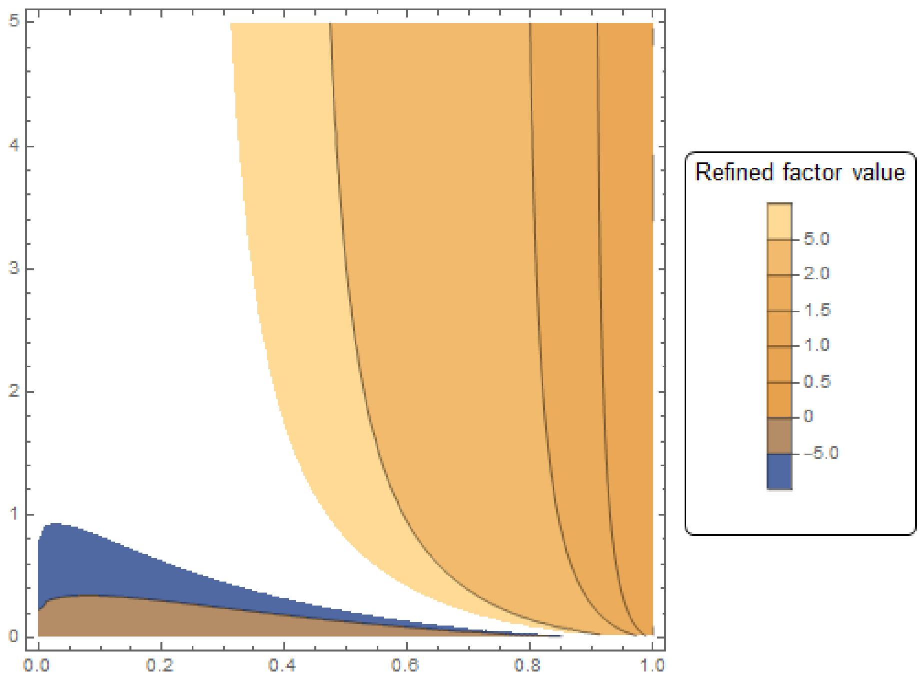

Figure 4.1: *Contour plot of the refined function. The flatness around the axes $x = 1$ can be used to estimate the effect of the refined approximation versus the simpler one.*

with threshold behavior:

$$r(x, \xi) \xrightarrow{x \to 1} 1, \qquad \forall \xi \tag{4.2.11}$$

The effect of choosing the refined approximation over the simpler one can be gauged by looking at how flat the function r is around $x = 1$, and how this flatness changes with ξ. Indeed this is a rough estimate of the magnitude of the power suppressed terms ($\mathcal{O}(1 - x)$ corrections) that are introduced by the new approximation. The contour plot for this function in the range $\xi \in (0, 5)$ is shown in Fig. 4.1.

We see that the refined function is relatively flat near the axes $x = 1$ even at low $p\perp$. It assumes values consistently different from 1 in the region $x \sim 0$, especially at low $p_\perp$, but this corresponds to high order power suppressed differences between the approximation.

For this reason we expect that the two approximation will not be substantially different in the medium N range, and will be almost identical in the large N region.

4.2.3 Kinematics for multiple gluon emissions

In this Section we analyze the kinematics of multiple gluon emission and give some degree of justification for the choice fo threshold function in the refined cross section Eq. (4.2.8). We will follow the kinematical analysis presented in Ref. [11] for the production of a prompt-photon, albeit considering a finite mass of the target particle.

We will assume that the reader is familiar with the notation introduced in Section 3.1 for the various kinematical quantities involved.

Analogously to the prompt-photon case, the threshold configurations for the production of an Higgs boson with fixed transverse momentum $p_\perp$ are the ones where each emitted gluon is either soft or collinear to the Higgs boson. Without loss of generality suppose that given $l+1$ gluon emissions the momenta $k_i = 1, ..., n$ are soft (with $n < l+1$) while the other gluons are collinear.

$$
\begin{aligned}
k_i =& 0, \qquad && 1 \le i \le n && (4.2.12)\\
k'_i \equiv k_{n+i} & \| p, \qquad && 1 \le i \le l+1-n = m+1 && (4.2.13)
\end{aligned}
$$

where obviously the transverse components of the collinear momenta have to sum up to the Higgs' transverse momentum:

$$
\sum_{i=1}^{m+1} k'_{i,\perp} = p_\perp \qquad (4.2.14)
$$

in order to ensure momentum conservation.

The phase space for such a process can be conveniently written as:

$$
\begin{aligned}
& d\varphi_{n+m+2}(p_1 + p_2; p, k_1, ..., k_n, k'_1, ..., k'_{m+1}) \\
& \qquad = \int_0^s \frac{dq^2}{2\pi} d\varphi_{n+1}(p_1 + p_2; q, k_1, ..., k_n) \times \\
& \qquad \times \int_0^{q^2} \frac{dk'^2}{2\pi} d\varphi_{m+1}(k', k'_1, ..., k'_{m+1}) d\varphi_2(q; p, k') \qquad (4.2.15)
\end{aligned}
$$

therefore decomposing it into a soft emission phase space $d\varphi_{n+1}$, a collinear emission phase space $d\varphi_{m+1}$ and a two particle phase space φ_2. A scheme of this decomposition is shown in figure 4.2.

The integration boundaries for q and k' needs to be refined further. It is easy to see that, in order for the production of an Higgs boson with transverse momentum $p_\perp$ to take place, one needs:

$$
xs < q^2 < s \qquad (4.2.16)
$$

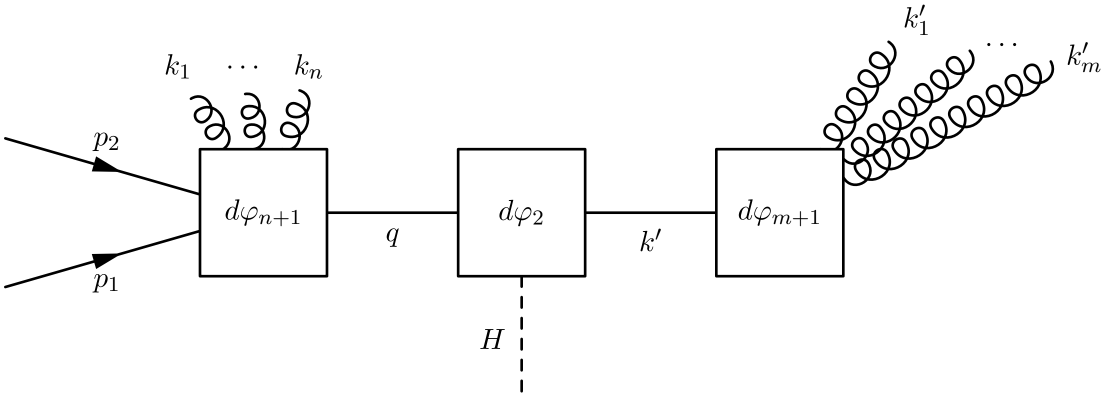

Figure 4.2: *Phase space decomposition for the emission of* n *soft gluons with momenta* $k_1, ..., k_n$ *and* m *collinear gluons with momenta* $k'_1, ..., k'_m$.

because xs is the minimum possible center-of-mass energy square necessary to produce the desired final state (i.e. an Higgs boson with the necessary extra radiation).

In order to identify the integration boundaries for k' we need to massage the two body phase space $d\varphi_2$:

$$\begin{aligned} d\varphi_2(q; k', p) =& \frac{d^{d-1}k'}{(2\pi)^{d-1}2k'_0} \frac{d^{d-1}p}{(2\pi)^{d-1}2E_H} (2\pi)^d \delta^{(d)}(q - k' - p) \\ =& \frac{(2\pi)^{2-d}}{4} \frac{d^{d-1}p}{k'_0 E_H} \delta(q_0 - k'_0 - E_H) \end{aligned} \tag{4.2.17}$$

where we exploited the Dirac delta to perform the $d^{d-1}k'$ integration. With the relations imposed by the "spacelike" delta we just used we can write the remaining, "timelike" delta as:

$$\delta(q_0 - k'_0 - E_H) = \delta(\sqrt{q^2} - \sqrt{|\overrightarrow{p}|^2 + k'^2} - \sqrt{|\overrightarrow{p}|^2 + m^2}) \tag{4.2.18}$$

where $\overrightarrow{p}$ is the spacelike $d-1$-momentum of the Higgs boson. By imposing that the argument of the Dirac delta be 0 and solving for $|\overrightarrow{p}|$ we obtain:

$$|\overrightarrow{p}| = \frac{q}{2} \left[\frac{\sqrt{(q^2 - k'^2 - m^2)^2 - 4k'^2 m^2}}{q^2} \right] \equiv P \tag{4.2.19}$$

where we only retained the positive solution.

It is also obvious that:

$$\frac{P}{p_\perp} = \frac{|\overrightarrow{p}|}{p_\perp} \geq 1 \tag{4.2.20}$$

and the equality is satisfied when the rapidity of the Higgs boson vanishes. Substituting Eq. (4.2.19) we obtain the inequality:

$$\begin{aligned}(2p_\perp q)^2 \leq &(q^2 - k'^2 - m^2)^2 - 4k'^2 m^2 \\ = &k'^4 - 2k'^2(q^2 + m^2) + (q^2 - m^2)^2\end{aligned} \tag{4.2.21}$$

Solving for k'^2 one finds the solutions:

$$k'^2 \leq k^2_{min} \cup k'^2 \geq k^2_{max} \tag{4.2.22}$$

$$k^2_{min,max} = (q^2 + m^2) \pm \sqrt{(q^2 + m^2)^2 + 4p_\perp^2 q^2 - (q^2 - m^2)^2} \tag{4.2.23}$$

The solutions $k'^2 \geq k^2_{max}$ are not acceptable since $k^2_{max} > q^2$, therefore after a little algebra we find for the range of k'^2:

$$0 \leq k'^2 \leq q^2 + m^2 - 2qm_\perp \tag{4.2.24}$$

Following the strategy adopted in the original paper[11] we define two new adimensional variables u and v:

$$k'^2 = v(q^2 + m^2 - 2qm_\perp) \tag{4.2.25}$$

$$q^2 = xs + u(s - xs) \tag{4.2.26}$$

$$0 \leq u, v \leq 1 \tag{4.2.27}$$

In the threshold limit we can therefore write:

$$k'^2 = vu(sx)\frac{1-a}{2}(1-x) + \mathcal{O}(1-x)^2 \tag{4.2.28}$$

$$q^2 = xs[1 + u(1-x)] + \mathcal{O}(1-x)^2 \tag{4.2.29}$$

$$\begin{aligned}P = &\frac{\sqrt{xs}}{2}\left[(1-a)^2 + \frac{1}{2}u(1-x)\left(1 - a^2 - v(1-3a)\right)\right] \\ &+ \mathcal{O}(1-x)^2\end{aligned} \tag{4.2.30}$$

where $a = a(\xi)$ was defined in Eq. (3.1.13).

We have checked that these expressions reduce to the ones obtained in Ref.[11] in the zero mass limit:

$$m \to 0 \quad \Rightarrow \quad a \to 0 \tag{4.2.31}$$

It was argued in the original paper[11] that the relevant scales for threshold resummation are:

$$k'^2 \propto (sx)\frac{1-a}{2}(1-x) \tag{4.2.32}$$

$$\frac{(s-q^2)^2}{q^2} \propto sx(1-x)^2 \tag{4.2.33}$$

Since the threshold logarithms will be logarithms of the ratio of two relevant scales, we can expect that the scale:

$$Q^2_{max} = s(1-x)\frac{1-a}{2} + \mathcal{O}(1-x)^2 \qquad (4.2.34)$$

will appear at every order in the threshold logarithms given the factor $(1-a)/2$ contained in k'^2.

Although this is not a complete proof for the exact form of the threshold logarithms, still it provides a reasonable argument for the choice of the refined logarithmic function L_2 in Eq. (4.2.8).

Chapter 5

Numerical results

In this Chapter we present some numerical results in order to verify the goodness of our approximation and to investigate the kinematical ranges of its applicability. All of the results shown refer to the production of a Higgs boson via gluon fusion.

The results are computed at the partonic level and in Mellin space. Since the hadronic cross section factorizes in the parton luminosity and the partonic cross section in Mellin space, it is possible to draw conclusions directly from the partonic cross sections, since the inclusion of the gluon PDFs only consists in a regular multiplication[1].

We will present all of our results as functions of N with $p_\perp$ fixed for three values of transverse momentum: $p_\perp = 10\text{GeV}$, 100GeV and 1000GeV. Since we were solely concerned with the threshold resummation and did not account for the large logarithms appearing at small $p_\perp$ we expect that our results will not be reliable at small $p_\perp$.

Finally we will plot all of the cross sections in units of σ_0, the LO inclusive cross section. In other words, we will be plotting the ratios:

$$R^i = \frac{1}{\sigma_0}\frac{d\sigma^i}{d\xi} \tag{5.0.1}$$

where i is whatever label indicating a specific cross section.

5.1 Numerical comparison at NLO

In this section we compare our approximations with the NLO full cross section and with the resummed cross section expanded at fixed order. The

[1] In direct space, instead, one needs to perform a convolution between the partonic cross sections and the PDFs and deriving qualitative statements directly from the partonic distribution in not straightforward.

comparison is performed at the level of partonic cross sections and in N space.

The resummed cross section expanded at fixed order is available in analytic form, Eq.(1.6.12); throughout this Section we will call this cross section simply *resummed cross section*, the pedantic reader may mentally add *expanded at fixed order* afterwards whenever this phrase is used.

On the other hand, our approximations are built in x space and then transformed to N space via a numerical Mellin transform, since a complete analytic Mellin transform is not available[1]. Finally, the full fixed order cross section is numerically integrated in rapidity and then transformed to N space, obviously with another numerical Mellin transform. We remind the reader that we are only considering the *singular* part of the NLO cross section, as defined in Eq.(3.2.6) following Glosser[4], and will continue to do so in this section.

Furthermore, we will only consider the II , IV and V terms in the NLO coefficient function Eq.(3.2.7) since all of the other terms are regular in the threshold region and we have no hope to approximate their contribution. This might be viewed as a trick to obtain a better match for our approximation. Indeed it is quite the opposite: every mismatch found in the plots shown can be directly pointed at as a failure of our approximation.

As already discussed in Section 4.1.3, we found a mismatch between the threshold coefficients of the resummed theory and those derived directly from the fixed order cross section. Since this Chapter is mainly focused on showing the effectiveness of our approximation, we are going to plot the resummed cross section expanded at fixed order as in Eq.(1.6.12) with the c coefficients matching the ones found for the fixed order cross section Eq.(4.1.23)-(4.1.25).

In Figure 5.1 the plots for the relevant cross section for fixed $p_\perp = 10\text{GeV}$ are shown.

As we expected, the two different approximations *soft1* (orange) and *soft2* (brown) are barely distinguished in the range shown. They both give a good approximation for the full cross section (light blue) for $N > 8$. What is more important, they surely approximate the full cross section better then the resummed result (light blue) does in the range $N > 5$.

[1] More precisely, the Mellin transform of the *soft1* approximation can actually be computed exactly, but the result contains an infinite sum. Therefore it is more convenient to perform the Mellin transform numerically.

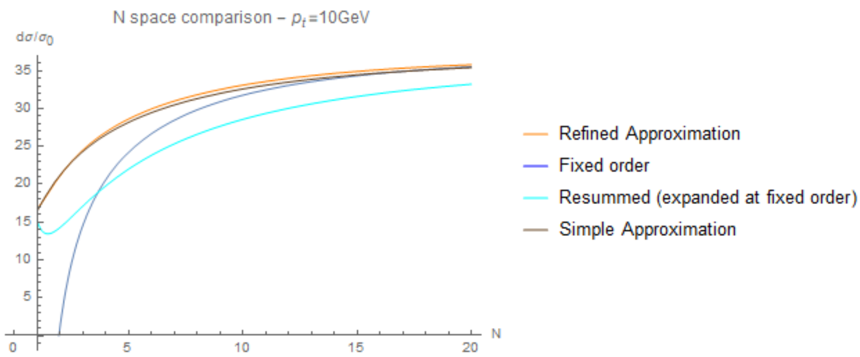

Figure 5.1: *Full cross section (blue), resummed cross section (light blue) and our approximations: soft1 (orange) and soft2 (brown). All of the cross sections are evaluated for fixed* $p_\perp = 10GeV$ *in the range* $N \in (1, 20)$.

Another important remark about Fig. 5.1 is that the resummed cross section does not converge to the full cross section nearly as fast as one would expect, given that it should correctly reproduce the threshold behavior of the full cross section.

This can be qualitatively addressed by the following argument: up to $\mathcal{O}(1-x)$ terms the full cross section has a global factor:

$$\frac{1}{\sqrt{(1-x)(1-a^2x)}} \tag{5.1.1}$$

which reproduces the LO threshold behavior. In the $p_\perp \to 0$ limit we have:

$$a(\xi) \to 1 \quad \Rightarrow \quad \frac{1}{\sqrt{(1-x)(1-a^2x)}} \to \frac{1}{1-x} \tag{5.1.2}$$

Therefore at $p_\perp = 0$ the logarithmic structure changes, in particular we expect logarithms one order higher then the ones appearing in the finite $p_\perp$ cross section. Our fixed order cross section does not contain all the contributions necessary to properly analyze the $p_\perp = 0$ case, but we expect that the inclusion of all the virtual Feynman diagrams with trivial $p_\perp$ distribution will lead to the regularization:

$$\frac{1}{1-x} + \text{virtual} \to \left(\frac{1}{1-x}\right)_+ \tag{5.1.3}$$

As is well known, this produces an extra power of threshold logarithms, see for example Ref. [9]. Therefore at $p_\perp = 0$ the resummed cross section is not expect to correctly reproduce the threshold behavior.

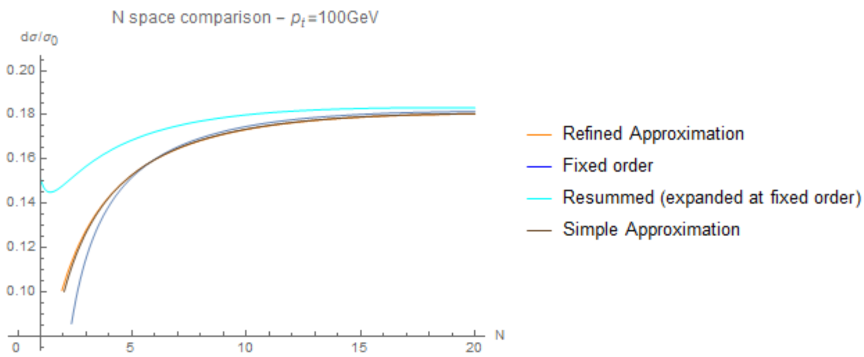

Figure 5.2: *Full cross section (blue), resummed cross section (light blue) and our approximations: soft1 (orange) and soft2 (brown). All of the cross sections are evaluated for fixed* $p_\perp = 100 GeV$ *in the range* $N \in (1, 20)$.

Since the transition between the two logarithm structures must occur continuously, we expect to see the effects even at small but finite $p_\perp$. This can be thought of as the fact that for small $p_\perp$ the factors φ_i in the expansion of the Hypergeometric function Eq. (C.2.6) become large. In the Mellin transform analysis used to link the threshold logarithms in x and N space we have discarded those terms, Eq. (B.3.5), because they are power suppressed. This is not a reliable approximation in the small $p_\perp$ region since, as we just shown, these subleading terms will grow end eventually give rise to an higher order logarithmic structure.

On the other hand, our approximations are built in x space, and the Mellin transform is performed numerically and therefore fully take into account the factor Eq. (5.1.1).

Then again, large logarithms of the form $\ln(Q^2/p_\perp)$ are known to appear in the fixed order cross section and since we have not properly resummed those, we do not trust our results in the small $p_\perp$ region, not even the full fixed order cross section.

In Figure 5.2 the corresponding results for $p_\perp = 100\text{GeV}$ are shown. Once again the two approximations *soft1* (orange) and *soft2* (brown) are almost indistinguishable. They give a good approximation to the fixed order cross section (blue) for $N > 5$ and an acceptable one even in the region $N > 3$.

On the other hand, the resummed cross section (light blue) can be considered a good approximation only for $N > 15$ and for $N < 8$ is completely unreliable. This reflects the fact that, as we have already discussed heavily, the resummed cross section has a wildly different low N behavior then the

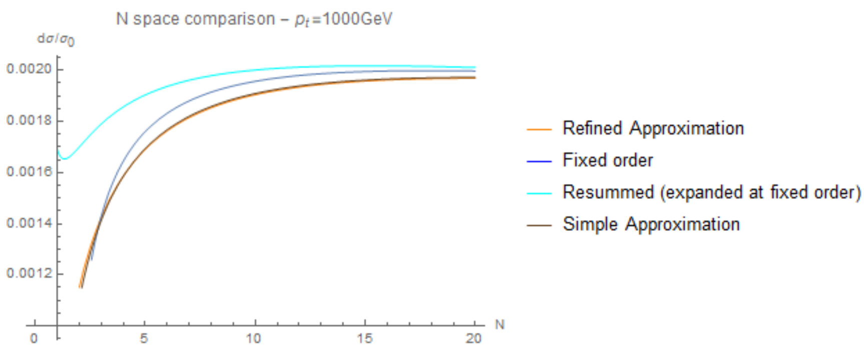

Figure 5.3: *Full cross section (blue), resummed cross section (light blue) and our approximations: soft1 (orange) and soft2 (brown). All of the cross sections are evaluated for fixed* $p_\perp = 1000 GeV$ *in the range* $N \in (1, 20)$.

fixed order one, exhibiting a different singularity structure (cuts instead of poles) in the unphysical ($N < 0$) region.

Finally Figure 5.3 contains the corresponding plot for fixed $p_\perp = 1000\text{GeV}$. The color correspondence for the various cross section is analogous to the ones adopted in the previous plots.

Once again the two approximations *soft1* and *soft2* are essentially indistinguishable. The matching of the approximations to the fixed order cross section is much worse than the one we found for $p_\perp = 100\text{GeV}$, still they provide an acceptable approximation. Is should also be noted that the cross section as a whole is much smaller then the one evaluated at $p_\perp = 100\text{GeV}$, peaking at 0.002 times σ_0.

Our approximations can be considered acceptable for $N > 3$ while once again the resummed cross section is only reliable in the $N > 10$ region. This can be explained with the same reasoning already used in the previous case $p_\perp = 100\text{GeV}$.

Generally speaking we can assert that our procedure provided us with a reliable approximation for the NLO fixed order $p_\perp$-distribution in the mid-high N region, roughly speaking for $N \sim 5$ onward, the precise interval depending on the transverse momentum. This is a considerable improvement with respect to the crude approximation derived from expanding at fixed order the resummed cross section.

Furthermore, despite our effort to provide a more refined version of our approximation via kinematical reasoning that has proven to improve the reliability in the case of inclusive cross section, the two approximations *soft1* and *soft2* do not appear to differ in a significant way and are at best distinguishable from each other. Since the difference between the fixed order cross section and both of our approximation is substantially greater then the difference between the approximations themselves in virtually all configurations, it does not seem useful to adopt the more complicated yet theoretically more promising refined approximation *soft2*. Adding subleading terms for the sake of adding subleading terms is never a good guide to useful results, therefore we will abandon the refined approximation from now on and only consider the *soft1* approximation, and we suggest future researchers to do the same.

Given the considerations just outlined we are confident in stating that: "*the soft approximation, built according to the procedure outlined in Chapter 4, is a reliable one in the medium and high N region and once matched to the known fixed order and (full) resummed cross section is expected to improve the overall theoretical accuracy of the $p_\perp$ distribution*".

Conclusion

In this thesis we have considered the $p_\perp$ distribution for the production of a colorless massive particle in hadron collisions. In particular we have analyzed the production of an Higgs boson in proton-proton collisions, which is one of the most relevant phenomena to be studied at hadronic colliders such as LHC.

We have analyzed the fixed order cross section in the threshold limit, i.e. when the center-of-mass energy of the incoming particles is just enough to produce an Higgs boson with a given transverse momentum, and the radiation necessary to recoil against it.

As is well known, the fixed order cross sections exhibits large logarithms of the form $\ln^k(1-x)$ where x is a threshold scaling variable, which become large in the threshold limit. These logarithms are usually resummed to all orders following resummation theory, which takes place in N space (Mellin space).

Since these logarithmic terms, once transformed to Mellin space, exhibit a pole singularity structure while the "resummed" logarithms $\ln N$ have a branch cut, the resummed cross section (and therefore its fixed order expansion) is not reliable in the small N region, which is far from threshold.

By constructing the explicit relations between direct space and Mellin space logarithms we were able to develop an approximation for the fixed order $p_\perp$ distribution, which reproduces the known threshold behavior computable from resummation theory while preserving the correct singularity structure (i.e. poles instead of branch cuts).

We outlined the procedure needed to build this approximation at all orders in perturbation theory and gave a justification for its reliability at higher orders, where the exact form of the large logarithms is not known.

We explicitly computed the approximation for the NLO $p_\perp$ distribution and compared it to the corresponding full fixed order cross section. The comparison showed that our approximation is reliable in the mid to high N region, for a wide range of transverse momenta. More importantly, our approximation is reliable in a range that is significantly larger with respect to the resummed cross section expanded at fixed order. This suggests that our approximation makes better use of the threshold information contained in the resummed result by simply matching the known singularity structure of the fixed order cross section.

Our approximation proved to be reliable roughly for $N \gtrsim 5$, with the exact interval depending on the transverse momentum. By contrast the resummed cross section expanded to fixed order was shown to be a reliable approximation only for $N \gtrsim 10$. The numerical results were presented and further commented in Chapter 5.

Furthermore, we built a refined version of our approximation by exploiting even more the kinematical structure of the multiple emission phase space. This enabled us to further specify the form of the threshold logarithms that are expected to appear at all orders in the perturbative expansion. Although theoretically more precise, at NLO this approximation did not exhibit a significantly different behavior with respect to the simpler one, to the point that it is impossible to identify which of the two approximations better matches the full fixed order cross section. We therefore concluded that the refinement did not bring any actual benefit and we limited ourselves to the simpler (and more easily justified) approximation.

Appendices

Appendix A

Plus Distributions

In this Appendix we review the basic notion of plus distribution and fix the notation used throughout this thesis. We also perform explicitly a change of variables for some particular distributions relevant to the computations performed in Chapter 3.

A.1 Definition and properties

We define two kinds of plus distributions which we will distinguish by using either round or square brackets. These are defined by their action on a generic Schwarz function[1]:

$$\int_0^1 (f(z))_+ g(z) \equiv \int_0^1 f(z)[g(z) - g(1)] \tag{A.1.1}$$

$$\int_0^1 [\zeta(q)]_+ \xi(q) \equiv \int_0^1 \zeta(q)[\xi(q) - \xi(0)] \tag{A.1.2}$$

These usually arise in QFT perturbative computation when there is a cancellation of divergences between real emission and virtual Feynman diagrams. Indeed the "round" plus distribution regularizes any function f that is divergent as $z \to 1$ at most as:

$$f(z) \sim (1-z)^{-\alpha}, \qquad \alpha < 2 \tag{A.1.3}$$

because the integral (A.1.1) is finite. Similarly the "square" plus distribution regularizes any function ζ that is divergent as $q \to 0$ at most as:

$$\zeta(q) \sim q^{-\alpha}, \qquad \alpha < 2 \tag{A.1.4}$$

This means that in order to distinguish which of the two definitions is being used it is usually enough to check whether the function f (or ζ) is

[1]A Schwarz function is a smooth function that decays sufficiently rapidly at infinity.

divergent as $z \to 1$ (or $q \to 0$), then it will be the "round" plus distribution (or the "square" plus distribution). In addition, throughout this thesis the "round" distributions will always depend on some variable named z or x while the "square" distributions will depend on q.

We wont review any other basic properties of plus distributions, the interested reader may find more informations in Ref.[9], Apeendix B for example.

A.2 Change of variable in plus distributions

In this section we explicitly compute the change of variables performed in Section 3.3.4; in doing so we will adopt some techniques found in Ref.[10]. Consider the distribution related to the function:

$$q^{-1+\varepsilon} \tag{A.2.1}$$

We wish to write a Taylor expansion in ε for this distribution near $\varepsilon = 0$ for $\varepsilon > 0$. We can write the action of this distribution on a generic function $\xi(q)$ as:

$$\begin{aligned}\int_0^1 q^{-1+\varepsilon}\xi(q)dq &= \int_0^1 q^{-1+\varepsilon}[\xi(q) - \xi(0)]dq + \xi(0)\int_0^1 q^{-1+\varepsilon}dq \\ &= \int_0^1 q^{-1+\varepsilon}[\xi(q) - \xi(0)]dq + \frac{\xi(0)}{\varepsilon}\end{aligned} \tag{A.2.2}$$

The we expand the $q^{-1+\varepsilon}$ in the last line in powers of ε up to $\mathcal{O}(\varepsilon)$, which is enough for the results needed in our computation.

$$q^{-1+\varepsilon} = \frac{1}{q}e^{\varepsilon \ln q} = \frac{1}{q} + \varepsilon\frac{\ln q}{q} + \mathcal{O}(\varepsilon^2) \tag{A.2.3}$$

Therefore we obtain:

$$\begin{aligned}\int_0^1 q^{-1+\varepsilon}\xi(q)dq = &\int_0^1 \frac{1}{q}[\xi(q) - \xi(0)]dq + \varepsilon\int_0^1 \frac{\ln q}{q}[\xi(q) - \xi(0)]dq \\ &+ \frac{\xi(0)}{\varepsilon} + \mathcal{O}(\varepsilon^2) \\ = &\int_0^1 \left(\left[\frac{1}{q}\right]_+ + \varepsilon\left[\frac{\ln(q)}{q}\right]_+ + \frac{\delta(q)}{\varepsilon}\right)\xi(q) + \mathcal{O}(\varepsilon^2)\end{aligned} \tag{A.2.4}$$

where we have used the definition of the "square" plus distribution Eq.(A.1.2). Abstracting from the integral we obtain the following relation between tempered distributions:

$$q^{-1+\varepsilon} = \frac{\delta(q)}{\varepsilon} + \left[\frac{1}{q}\right]_+ + \left[\frac{\ln(q)}{q}\right]_+ + \mathcal{O}(\varepsilon^2) \tag{A.2.5}$$

We have now related two plus distributions in the variable q to the function $q^{-1+\varepsilon}$. Since this is an ordinary function there is no subtlety involved in changing its variable. In particular we are interested in the change obtained from inverting Eqs.(3.2.10), (3.3.12):

$$q = \frac{-t}{Q^2_{max}} \frac{1-z_t}{z_t} \tag{A.2.6}$$

and analogously for u. We obtain:

$$q^{-1+\varepsilon} = \left(\frac{-t}{Q^2_{max} z_t}\right)^{-1+\varepsilon} (1-z_t)^{-1+\varepsilon} \tag{A.2.7}$$

We can expand $(1-z_t)^{-1+\varepsilon}$ as a power series in a similar way to what we did with $q^{-1+\varepsilon}$, essentially writing it in terms of "round" plus distributions. The full computation can be found in Ref.[10] or can be considered as a simple exercise; the final result enables us to write:

$$q^{-1+\varepsilon} = \left(\frac{-t}{Q^2_{max} z_t}\right)^{-1+\varepsilon} \left[\frac{\delta(1-z_t)}{\varepsilon} + \left(\frac{1}{1-z_t}\right)_+ + \varepsilon \left(\frac{\ln(1-z_t)}{1-z_t}\right)_+ + \mathcal{O}(\varepsilon^2)\right] \tag{A.2.8}$$

The two Taylor expansions Eqs.(A.2.5), (A.2.8) must obviously be equal, in particular every coefficient in the ε expansion must coincide. From comparing the ε^{-1} coefficients we immediately obtain:

$$\delta(q) = \frac{Q^2_{max}}{-t} \delta(1-z_t) \tag{A.2.9}$$

which could have been derived via standard computations, exploiting the properties of the Dirac delta under a change of variable. Substituting Eq.(A.2.9) into Eq.(A.2.8) and expanding the factor $(-t/Q^2_{max} z_t)^{-1+\varepsilon}$ up to $\mathcal{O}(\varepsilon)$ we get:

$$\begin{aligned} q^{-1+\varepsilon} =& \frac{\delta(q)}{\varepsilon} + \delta(q) \ln \frac{-t}{Q^2_{max}} + \frac{Q^2_{max} z_t}{-t} \left(\frac{1}{1-z_t}\right)_+ \\ &+ \varepsilon \left\{ \frac{\delta(q)}{2} \ln^2 \frac{-t}{Q^2_{max}} + \frac{Q^2_{max} z_t}{-t} \left[\ln \frac{-t}{Q^2_{max} z_t} \left(\frac{1}{1-z_t}\right)_+ + \left(\frac{\ln(1-z_t)}{1-z_t}\right)_+ \right] \right\} \\ &+ \mathcal{O}(\varepsilon^2) \end{aligned} \tag{A.2.10}$$

Now we can compare the two power expansions of $q^{-1+\varepsilon}$ order by order. This comparison up to $\mathcal{O}(\varepsilon)$ enables us to write the two plus distributions we are interested in, Eqs.(3.3.16), in terms of "square" plus distributions depending on q. We obtain:

$$\frac{z_t}{-t}\left(\frac{1}{1-z_t}\right)_+ = \frac{1}{Q^2_{max}}\left\{\left[\frac{1}{q}\right]_+ + \delta(q)\ln\frac{Q^2_{max}}{-t}\right\} \tag{A.2.11}$$

$$\begin{aligned}\frac{z_t}{-t}\left(\frac{\ln(1-z_t)}{1-z_t}\right)_+ = \frac{1}{Q^2_{max}}\Big\{&\left[\frac{\ln(q)}{q}\right]_+ + \ln\frac{Q^2_{max}z_t}{-t}\left[\frac{1}{q}\right]_+ \\ &+\frac{\delta(q)}{2}\ln^2\frac{Q^2_{max}}{-t}\Big\}\end{aligned} \tag{A.2.12}$$

Generally speaking this procedure could be extended to any plus distribution of the form:

$$\left(\frac{\ln^k(1-z)}{1-z}\right) \tag{A.2.13}$$

simply by expanding the function $q^{-1+\varepsilon}$ up to $\mathcal{O}(\varepsilon^k)$.

A.3 q integration of logarithmic plus distributions

In this section we will tackle the fundamental q integrals needed to obtain the NLO fixed order $p_\perp$ distribution from the double differential one. These are integrals of the form:

$$\int_0^1 \left[\frac{1}{q}\right]_+ \frac{1}{\sqrt{(1-q)}}dq \tag{A.3.1}$$

$$\int_0^1 \left[\frac{\ln(q)}{q}\right]_+ \frac{1}{\sqrt{(1-q)}}dq \tag{A.3.2}$$

although the procedure used in their computation can be straightforwardly extended to any integral of the form:

$$\int_0^1 \left[\frac{\ln^k q}{q}\right]_+ \frac{1}{\sqrt{(1-q)}}dq \tag{A.3.3}$$

Define the generating integral (for $\varepsilon > 0$):

$$\begin{aligned}I_\varepsilon =& \int_0^1 \frac{1}{q^{-1+\varepsilon}}\left[\frac{1}{\sqrt{(1-q)}} - 1\right] \\ =&\beta\left(\varepsilon, \frac{1}{2}\right) - \frac{1}{\varepsilon} \\ =&\frac{\Gamma\left(\frac{1}{2}\right)\Gamma(\varepsilon)}{\Gamma\left(\frac{1}{2}+\varepsilon\right)} - \frac{1}{\varepsilon}\end{aligned} \tag{A.3.4}$$

where β is Euler's beta function. From the generating integral we can extract the integrals we are interested in by differentiating with respect to ε:

$$\int_0^1 \left[\frac{\ln^k(q)}{q}\right]_+ \frac{1}{\sqrt{(1-q)}} dq = \left.\frac{d^k I_\varepsilon}{d\varepsilon^k}\right|_{\varepsilon=0} \tag{A.3.5}$$

In order to compute the integrals (A.3.1)-(A.3.2) we will only need to compute I_ε up to $\mathcal{O}(\varepsilon)$ as a partial Taylor expansion near $\varepsilon = 0$. Using the Taylor expansions of the beta function Eq.(C.1.7):

$$\begin{aligned}
I_\varepsilon = \;& \psi_0(1) - \psi_0\left(\frac{1}{2}\right) \\
& + \varepsilon\Big[\frac{1}{2}\psi_0^2\left(\frac{1}{2}\right) + \frac{1}{2}\left(\psi_1(1) + \psi_0^2(1)\right) \\
& - \frac{1}{2}\psi_1\left(\frac{1}{2}\right) - \psi_0(1)\psi_0\left(\frac{1}{2}\right)\Big] \\
& + \mathcal{O}(\varepsilon^2) && \text{(A.3.6)} \\
= \;& \Theta_1 + \varepsilon\Theta_2 + \mathcal{O}(\varepsilon^2) && \text{(A.3.7)}
\end{aligned}$$

Where we have defined for notational convenience:

$$\Theta_1 = \psi_0(1) - \psi_0\left(\frac{1}{2}\right) \tag{A.3.8}$$

$$\Theta_2 = \frac{1}{2}\psi_0^2\left(\frac{1}{2}\right) + \frac{1}{2}\left(\psi_1(1) + \psi_0^2(1)\right) - \frac{1}{2}\psi_1\left(\frac{1}{2}\right) - \psi_0(1)\psi_0\left(\frac{1}{2}\right) \tag{A.3.9}$$

Then the integrals (A.3.1)-(A.3.2) are:

$$\int_0^1 \left[\frac{1}{q}\right]_+ \frac{1}{\sqrt{(1-q)}} dq = \Theta_1 \tag{A.3.10}$$

$$\int_0^1 \left[\frac{\ln(q)}{q}\right]_+ \frac{1}{\sqrt{(1-q)}} dq = \Theta_2 \tag{A.3.11}$$

Appendix B

Mellin Transform

In this Appendix we review the Mellin transform, showing some basic facts and computing the transform of some some functions of interest in the context of $p_\perp$ distributions.

B.1 Definition and properties

The Mellin transform of a function $f(x)$ defined on the interval $0 < x < 1$ is defined as:

$$\tilde{f}(N) = \mathcal{M}\left[f(x)\right](N) = \int_0^1 x^{N-1} f(x) dx \tag{B.1.1}$$

As is customary, we will immediately drop the tilde on top of the transformed function and distinguish the function $f(x)$ from its Mellin transform simply through their arguments. It can be shown that if the Mellin transform of a function exists, then it is analytic for $\mathrm{Re}(N) > k$ for some real number k depending on $f(x)$.

For the Mellin transform of a physical quantity, for example a cross section, the region $\mathrm{Re}(N) > k$ where the integral Eq.(B.1.1) is actually defined is usually called the *physical region.*

It is customary to exploit the analyticity of $f(N)$ in the half plane $\mathrm{Re}(N) > k$ to analytically continue it to the whole complex plane, with the exception of eventual singularities.

The inverse Mellin transform can be computed as:

$$f(x) = \frac{1}{2\pi i} \int_{c+i\infty}^{c-i\infty} x^{-N} f(N) dN \tag{B.1.2}$$

Where c is some real constant greater then k, thus rendering the contour of the integral in Eq.(B.1.2) a straight line parallel to the imaginary axes which lies to the right of the rightmost singularity of $f(N)$. The integration contour can actually be deformed at will as long as it does not cross any singularity.

Consider now the multiplicative convolution $\otimes$ as defined in:

$$(f \otimes g)(x) \equiv \int_x^1 \frac{dy}{y} f(y) g\left(\frac{x}{y}\right) \tag{B.1.3}$$

$$= \int_0^1 dy \int_0^1 dz f(y) g(z) \delta(x - yz) \tag{B.1.4}$$

As can be easily check from the second equality Eq.(B.1.4), the multiplicative convolution factorizes upon Mellin transformation:

$$\mathcal{M}\left[f \otimes g\right](N) = \mathcal{M}\left[f\right](N) \cdot \mathcal{M}\left[g\right](N) \tag{B.1.5}$$

A final general property which can be checked directly from the definition of the Mellin transform is:

$$\mathcal{M}\left[x f(x)\right](N) = \mathcal{M}\left[f(x)\right](N+1) \tag{B.1.6}$$

thus multiplying $f(x)$ by any polynomial of x will amount to a series of terms which are obtained simply by translating $f(N)$ by integers.

B.2 Mellin transform of plus distribution and asymptotic behavior

Although we are not interested in taking the Mellin transform of plus distributions, as this operation is never required throughout the computations performed in this thesis, it is still useful to be able to tackle these transformations since they frequently appear in the computation of cross section, for example in the computation of the inclusive cross section in Mellin space.

From the definition of the plus distribution Eq.(A.1.1) we can write:

$$\mathcal{M}\left[(f)_+(x)\right](N) = \int_0^1 f(x) \left[x^{N-1} - 1\right] \tag{B.2.1}$$

The Mellin transform of a plus distribution has a qualitatively different behavior in the $|N| \to \infty$ limit. Indeed from the first Riemann-Lebesgue lemma it can be proven that for a regular function $h(x)$ ($h \in L_1([0,1])$):

$$\lim_{N\to\infty} \mathcal{M}\left[h(x)\right](N) = 0 \tag{B.2.2}$$

The same limit for the Mellin transform of a plus distribution is quite different. Indeed it can be proven that[1]:

$$|\mathcal{M}\left[(f)_+(N)\right]| \xrightarrow{N\to\infty} \left|\int_0^1 dz f(z)\right| \tag{B.2.3}$$

Then, depending on how the function f behaves in the $x \sim 1$ region we may have different results for the large N limit. Suppose that f diverges as $(1-x)^{-\alpha}$, we have:

$$\alpha < 1 \quad \rightarrow \quad \lim_{N\to\infty} \mathcal{M}\left[(f)_+\right](N) = \left|\int_0^1 dz f(z)\right| \in \mathbb{R}^+ \tag{B.2.4}$$

$$1 \leq \alpha < 2 \quad \rightarrow \quad \lim_{N\to\infty} \mathcal{M}\left[(f)_+\right](N) = \infty \tag{B.2.5}$$

$$\alpha \geq 2 \quad \rightarrow \quad \text{Plus distribution not well defined} \tag{B.2.6}$$

Let us make a couple of relevant examples. The fixed order inclusive cross section for Higgs production contains plus distributions of the form[2]:

$$\left(\frac{\ln^k(1-x)}{1-x}\right) \tag{B.2.7}$$

These clearly fall into the second category just described, being that they diverge as $(1-x)^{-1}$ as $x \to 1$. Therefore their Mellin transform will be divergent in the $N \to \infty$ limit, indeed it can be seen that they diverge logarithmically.

Instead, the fixed order $p_\perp$ distribution diverges as:

$$\frac{\ln^k(1-x)}{\sqrt{1-x}} \tag{B.2.8}$$

Since we have not included all of the virtual diagrams we don't see any plus distribution arising, but a full fixed order computation will contain the corresponding plus distributions:

$$\left(\frac{\ln^k(1-x)}{\sqrt{1-x}}\right)_+ \tag{B.2.9}$$

as can be seen for example in the full LO $p_\perp$ distribution derived in Ref. [8], Equation (1.3.30). These fall into the first category (since here $\alpha = 1/2$) and their Mellin transform will be finite in the $N \to \infty$ limit.

[1] See for example Ref. [9], Appendix B.
[2] See for example Eq. (3.3.11).

B.3 Mellin transform of the $p_\perp$-spectrum threshold logarithms

In this section we compute the Mellin transform of the logarithmic terms appearing in the threshold region in the NLO $p_\perp$ distribution Eq.(3.5.12).

We are interested in the following integrals:

$$D_k^a(N) \equiv \int_0^1 \frac{x^N}{\sqrt{(1-x)(1-ax)}} \ln^k(1-x)dx \tag{B.3.1}$$

for $k = 0, 1, 2$. These can be evaluated from the generating integral:

$$D_\eta^a(N) \equiv \int_0^1 \frac{x^N}{\sqrt{(1-x)(1-ax)}}(1-x)^\eta dx \tag{B.3.2}$$

by differentiating with respect to η:

$$D_k^a(N) = \left. \frac{d^k D_\eta^a(N)}{d\eta^k} \right|_{\eta=0} \tag{B.3.3}$$

The generating interal $D_\eta^a(N)$ is easily evaluated as a special case of the Euler representation of the Hypergeometric Function ${}_2F_1$, Eq.(C.2.4).

$$\begin{aligned} D_\eta^a(N) =& \frac{\Gamma(N)\,\Gamma\left(\eta+\frac{1}{2}\right)}{\Gamma\left(N+\eta+\frac{1}{2}\right)}\, {}_2F_1\left(\frac{1}{2}, N; N+\eta+\frac{1}{2}; a^2\right) \\ =& D_0^a(N) \frac{\Gamma\left(\frac{1}{2}+\eta\right)}{\Gamma\left(\frac{1}{2}\right)} \frac{\Gamma\left(N+\frac{1}{2}\right)}{\Gamma\left(N+\frac{1}{2}+\eta\right)} \frac{{}_2F_1\left(\frac{1}{2}, N; N+\eta+\frac{1}{2}; a^2\right)}{{}_2F_1\left(\frac{1}{2}, N; N+\frac{1}{2}; a^2\right)} \end{aligned} \tag{B.3.4}$$

where we have factorized out $D_0^a(N) = D_\eta^a(N)|_{\eta=0}$.

In order to obtain the explicit formula for $D_k^a(N)$ (for $k = 0, 1, 2$) it is sufficient to evaluate (B.3.4) as a series expansion in η up to $\mathcal{O}(\eta^2)$. In order to do this, we can exploit the power expansion for the ratios of Gamma functions Eq.(C.1.6) (and the corresponding power expansion for its inverse) and that of the ratio of Hypergemotric functions, in particular the fact that:

$$\frac{{}_2F_1\left(\frac{1}{2}, N; N+\eta+\frac{1}{2}; a^2\right)}{{}_2F_1\left(\frac{1}{2}, N; N+\frac{1}{2}; a^2\right)} = 1 + \mathcal{O}\left(\frac{1}{N}\right) \tag{B.3.5}$$

With a little algebra we obtain:

$$\frac{D_\eta^a(N)}{D_0^a(N)} = 1$$

$$
\begin{aligned}
&+ \eta \left[\psi_0 \left(\frac{1}{2} \right) - \psi_0 \left(N + \frac{1}{2} \right) \right] \\
&+ \frac{\eta^2}{2} \left[\psi_0^2 \left(\frac{1}{2} \right) + \psi_0^2 \left(N + \frac{1}{2} \right) + \psi_1 \left(\frac{1}{2} \right) - \psi_1 \left(N + \frac{1}{2} \right) \right. \\
&\qquad \left. -2\psi_0 \left(\frac{1}{2} \right) \psi_0 \left(N + \frac{1}{2} \right) \right] \\
&+ \mathcal{O}(\eta^3) + \mathcal{O}\left(\frac{1}{N} \right)
\end{aligned} \tag{B.3.6}
$$

In the large N limit we can also exploit the asymptotic behaviour of the Poligamma functions, namely $\psi_0(N) \sim \ln(N)$ and $\psi_1 \sim 1/N$:

$$
\begin{aligned}
\frac{D_\eta^a(N)}{D_0^a(N)} &= 1 + \eta \left[\psi_0 \left(\frac{1}{2} \right) - \ln(N) \right] \\
&+ \frac{\eta^2}{2} \left[\psi_0^2 \left(\frac{1}{2} \right) + \ln^2(N) + \psi_1 \left(\frac{1}{2} \right) - 2\psi_0 \left(\frac{1}{2} \right) \ln(N) \right] \\
&+ \mathcal{O}(\eta^3) + \mathcal{O}\left(\frac{1}{N} \right)
\end{aligned} \tag{B.3.7}
$$

Now computing the specific integrals $D_k^a(N)$ is just a matter of extracting the coefficients of this expansion, factoring out the $1/k!$. Our expansion up to $\mathcal{O}(\eta^2)$ enables us to compute these integrals up to $k = 2$, but it is easy to see how this procedure can be straightforwardly extended to any k. We obtain:

$$
D_0^a(N) = \frac{\Gamma(N)\,\Gamma\left(\eta + \frac{1}{2}\right)}{\Gamma\left(N + \eta + \frac{1}{2}\right)} \, {}_2F_1\left(\frac{1}{2}, N; N + \frac{1}{2}; a^2 \right) \tag{B.3.8}
$$

$$
D_1^a(N) = D_0^a(N) \left[\psi_0 \left(\frac{1}{2} \right) - \ln(N) + \mathcal{O}\left(\frac{1}{N} \right) \right] \tag{B.3.9}
$$

$$
\begin{aligned}
D_2^a(N) = D_0^a(N) \Bigg[&\psi_0^2 \left(\frac{1}{2} \right) + \ln^2(N) + \psi_1 \left(\frac{1}{2} \right) \\
&- 2\psi_0 \left(\frac{1}{2} \right) \ln(N) + \mathcal{O}\left(\frac{1}{N} \right) \Bigg]
\end{aligned} \tag{B.3.10}
$$

Appendix C

Special Functions

In this Appendix we review some special functions arising during the calculations performed in this thesis.

C.1 Euler Gamma and Poligamma functions

The Euler Gamma function can be defined in the complex plane as:

$$\Gamma(z) = \int_0^\infty dt e^{-t} t^{z-1}, \qquad Re(z) > 0 \tag{C.1.1}$$

Integrating by parts it can be shown that the Gamma function satisfies the fundamental property:

$$\Gamma(z+1) = z\Gamma(z) \tag{C.1.2}$$

therefore essentially being a natural extension of the factorial in the complex plane, in particular:

$$\Gamma(n+1) = n!, \qquad n \in \mathbb{N} \tag{C.1.3}$$

Equation (C.1.2) can be used to analytically extend the domain of the Gamma function to the whole complex plane, with the exception of a series of single poles located at the non positive integer numbers. Around any point ζ which is not a pole the Gamma function satisfies the Taylor expansion:

$$\Gamma(\zeta + \varepsilon) = \Gamma(\zeta) \left[1 + \varepsilon \psi_o(\zeta) + \frac{\varepsilon^2}{2} \left(\psi_1(\zeta) + \psi_0^2(\zeta) \right) + \mathcal{O}(\varepsilon^3) \right] \tag{C.1.4}$$

where ψ_i are the Poligamma functions defined in Eq.(C.1.8).

By setting $\zeta = 1$ in Eq.(C.1.4) and exploiting the fundamental property of the Gamma function we can derive the Laurent expansion around $z = 0$:

$$\Gamma(\varepsilon) = \frac{\Gamma(1+\varepsilon)}{\varepsilon} = \frac{1}{\varepsilon} + \psi_0(1) + \frac{\varepsilon}{2} \left(\psi_1(1) + \psi_0^2(1) \right) + \mathcal{O}(\varepsilon^2) \tag{C.1.5}$$

Another useful power expansion we are going to use is:

$$\frac{\Gamma(\zeta)}{\Gamma(\zeta+\varepsilon)} = 1 - \varepsilon\psi_0(\zeta) + \frac{\varepsilon^2}{2}\left(\psi_0^2(\zeta) - \psi_1(\zeta)\right) + \mathcal{O}(\varepsilon^2) \tag{C.1.6}$$

Finally we can derive an useful expansion of the Euler Beta function, which is used in Appendix A for the computation of a generating integral.

$$\begin{aligned}\beta\left(\varepsilon, \frac{1}{2}\right) =&\frac{\Gamma\left(\frac{1}{2}\right)\Gamma\left(\varepsilon\right)}{\Gamma\left(\frac{1}{2}+\varepsilon\right)} \\ =&\frac{1}{\varepsilon} + \psi_0(1) - \psi_0\left(\frac{1}{2}\right) \\ &+ \varepsilon\Big[\frac{1}{2}\psi_0^2\left(\frac{1}{2}\right) + \frac{1}{2}\left(\psi_1(1) + \psi_0^2(1)\right) \\ &\qquad - \frac{1}{2}\psi_1\left(\frac{1}{2}\right) - \psi_0(1)\psi_0\left(\frac{1}{2}\right)\Big] \\ &+ \mathcal{O}(\varepsilon^2)\end{aligned} \tag{C.1.7}$$

The Poligamma functions are defined as logarithmic derivatives of the Gamma function:

$$\psi_k(z) = \frac{d^{k+1}}{dz^{k+1}}\ln\Gamma(z) \tag{C.1.8}$$

The Poligamma function with $k = 0$ is usually called Digamma function and denoted as ψ, without any subscript. For large $|z|$ and with $\arg z < \pi$ the Poligamma functions behave as:

$$\psi_0(z) \simeq \ln z + \mathcal{O}\left(\frac{1}{z}\right) \tag{C.1.9}$$

$$\psi_i(z) =\mathcal{O}\left(\frac{1}{z^i}\right), \qquad i > 0 \tag{C.1.10}$$

C.2 Hypergeometric Function

The (p, q) Hypergeometric function is defined as:

$${}_pF_q(a_1, ..., a_p; b_1, ..., b_q; z) \equiv \sum_{k=0}^{\infty} \frac{(a_1)_k...(a_p)_k}{(b_1)_k...(b_q)_k}\frac{z^k}{k!} \tag{C.2.1}$$

where $(a)_k$ is the Pochhammer symbol defined as:

$$(a)_k = \frac{\Gamma(a+k)}{\Gamma(a)} = a(a+1)\cdots(a+k-1) \tag{C.2.2}$$

These are a class of very general functions which contains many other special (and ordinary) functions as special cases. We will be interested in the $(2,1)$ Hypergeometric Function:

$$
{}_2F_1(a,b;c;z) = \sum_{k=0}^{\infty} \frac{(a)_k (b)_k}{(c)_k} \frac{z^k}{k!} \tag{C.2.3}
$$

because it appears in the evaluation of the Euler-Type integral:

$$
\int_0^1 x^b (1-x)^c (1-zx)^{-a} dx = \beta(b+1, c+1)\, {}_2F_1(a,b;c;z) \tag{C.2.4}
$$

which is well defined if z is not a real number greater or equal to 1, which will always be the case in our computation. Equation (C.2.4) can be proven by expanding $(1-zx)^{-a}$ and then performing the integration term by term thanks to the ordinary Euler Beta function integral.

In particular, in the computation of the Mellin transform of the fixed order cross section we will encounter the function:

$$
{}_2F_1\left(\frac{1}{2}, N; N+\eta+\frac{1}{2}; a^2\right) \tag{C.2.5}
$$

which we would like to expand in powers of η. The expansion up to $\mathcal{O}(\eta^2)$ can be written as:

$$
\begin{aligned}
\frac{{}_2F_1\left(\frac{1}{2}, N; N+\eta+\frac{1}{2}; a^2\right)}{{}_2F_1\left(\frac{1}{2}, N; N+\frac{1}{2}; a^2\right)} =& 1 + \eta\varphi_0(N,a^2) \\
&+ \frac{\eta^2}{2}\left(\varphi_1(N,a^2) + \varphi_0^2(N,a^2)\right) + \mathcal{O}(\eta^3) \qquad \text{(C.2.6)}
\end{aligned}
$$

where φ_i are the logarithmic derivatives of the Hypergeometric function Eq.(C.2.5) with respect to η:

$$
\varphi_k(N,a^2) \equiv \frac{d^{(k+1)}}{d\eta^{(k+1)}} \ln\left({}_2F_1\left(\frac{1}{2}, N; N+\eta+\frac{1}{2}; a^2\right)\right)_{\eta=0} \tag{C.2.7}
$$

In can be shown that each of these logarithmic derivative vanish at least as $1/N$ in the $N \to \infty$ limit. This is because the derivative of a Pochhammer symbol $(a)_k$ with respect to its argument is a polynomial of degree $k-1$, which is one degree less then the symbol itself[19]. Without focusing too much on the precise asymptotics of these functions we limit ourselves to a weaker statement, which is enough for our purposes nevertheless:

$$
\varphi_k(N,a^2) \xrightarrow{N\to\infty} 0 \tag{C.2.8}
$$

Bibliography

[1] R. D. Ball, M. Bonvini, S. Forte, S. Marzani and G. Ridolfi, "Higgs production in gluon fusion beyond NNLO," Nucl. Phys. B **874** (2013), 746-772 doi:10.1016/j.nuclphysb.2013.06.012 [arXiv:1303.3590 [hep-ph]].

[2] G. Aad *et al.* [ATLAS], "Observation of a new particle in the search for the Standard Model Higgs boson with the ATLAS detector at the LHC," Phys. Lett. B **716** (2012), 1-29 doi:10.1016/j.physletb.2012.08.020 [arXiv:1207.7214 [hep-ex]].

[3] C. J. Glosser, "Higgs boson production in hadron hadron colliders," [arXiv:hep-ph/0201054 [hep-ph]].

[4] C. J. Glosser and C. R. Schmidt, "Next-to-leading corrections to the Higgs boson transverse momentum spectrum in gluon fusion," JHEP **12** (2002), 016 doi:10.1088/1126-6708/2002/12/016 [arXiv:hep-ph/0209248 [hep-ph]].

[5] V. Ravindran, J. Smith and W. L. Van Neerven, "Next-to-leading order QCD corrections to differential distributions of Higgs boson production in hadron hadron collisions," Nucl. Phys. B **634** (2002), 247-290 doi:10.1016/S0550-3213(02)00333-4 [arXiv:hep-ph/0201114 [hep-ph]].

[6] D. de Florian, A. Kulesza and W. Vogelsang, "Threshold resummation for high-transverse-momentum Higgs production at the LHC," JHEP **02** (2006), 047 doi:10.1088/1126-6708/2006/02/047 [arXiv:hep-ph/0511205 [hep-ph]].

[7] R. Bonciani, S. Catani, M. L. Mangano and P. Nason, "Sudakov resummation of multiparton QCD cross-sections," Phys. Lett. B **575** (2003), 268-278 doi:10.1016/j.physletb.2003.09.068 [arXiv:hep-ph/0307035 [hep-ph]].

[8] C. Muselli, "Resummation of transverse momentum distributions," unpublished thesis, PHD thesis, 2017

[9] M. Bonvini, "Resummation of soft and hard gluon radiation in perturbative QCD," [arXiv:1212.0480 [hep-ph]].

[10] B. Pötter, "Calculational techniques in perturbative QCD: the Drell-Yan process," unpublished notes, 1997

[11] P. Bolzoni, S. Forte and G. Ridolfi, "Renormalization group approach to Sudakov resummation in prompt photon production," Nucl. Phys. B **731** (2005), 85-108 doi:10.1016/j.nuclphysb.2005.07.036 [arXiv:hep-ph/0504115 [hep-ph]].

[12] S. Forte and G. Ridolfi, "Renormalization group approach to soft gluon resummation," Nucl. Phys. B **650** (2003), 229-270 doi:10.1016/S0550-3213(02)01034-9 [arXiv:hep-ph/0209154 [hep-ph]].

[13] W. Bizon, P. F. Monni, E. Re, L. Rottoli and P. Torrielli, "Momentum-space resummation for transverse observables and the Higgs $p_\perp$ at N^3LL+NNLO," JHEP **02** (2018), 108 doi:10.1007/JHEP02(2018)108 [arXiv:1705.09127 [hep-ph]].

[14] M. Spira, A. Djouadi, D. Graudenz and P. M. Zerwas, "Higgs boson production at the LHC," Nucl. Phys. B **453** (1995), 17-82 doi:10.1016/0550-3213(95)00379-7 [arXiv:hep-ph/9504378 [hep-ph]].

[15] R. V. Harlander and W. B. Kilgore, "Next-to-next-to-leading order Higgs production at hadron colliders," Phys. Rev. Lett. **88** (2002), 201801 doi:10.1103/PhysRevLett.88.201801 [arXiv:hep-ph/0201206 [hep-ph]].

[16] C. Anastasiou and K. Melnikov, "Higgs boson production at hadron colliders in NNLO QCD," Nucl. Phys. B **646** (2002), 220-256 doi:10.1016/S0550-3213(02)00837-4 [arXiv:hep-ph/0207004 [hep-ph]].

[17] S. Weinberg, "Infrared photons and gravitons," Phys. Rev. **140** (1965), B516-B524 doi:10.1103/PhysRev.140.B516

[18] A. Strominger, "Lectures on the Infrared Structure of Gravity and Gauge Theory," [arXiv:1703.05448 [hep-th]].

[19] D. Greynat, J. Sesma and G. Vulvert, "Derivatives of the Pochhammer and reciprocal Pochhammer symbols and their use in epsilon-expansions of Appell and Kampé de Fériet functions," J. Math. Phys. **55** (2014), 043501 doi:10.1063/1.4870619

[20] R. K. Ellis, W. J. Sirling and B. R. Webber, *QCD and Collider Physics*, Cambridge Univ. Press, Cambridge, 2004.